

~~CONFIDENTIAL~~

24

NASA TECHNICAL
MEMORANDUM

NASA TM X-53041

MAY 1, 1964

N74-71467

4/5p
(NASA-TM-X-53041) RIGID BODY STUDY OF
CONTROL, SEPARATION, AND LIFT-OFF FOR
SA-6 VEHICLE (NASA) 45 p

Unclas

00/99 28406

Vol 2

NASA TM X-53041

CLASSIFIED
TO - UNCLASSIFIED
By authority of E.O. 11652
Changed by L. Shirley Date 1-18-74

RIGID BODY STUDY OF CONTROL, SEPARATION, AND LIFT-OFF FOR SA-6 VEHICLE (v)

by E. L. SULLIVAN, D. O. McNIEL AND W. H. HARMON
Aero-Astroynamics Laboratory

NASA

*George C. Marshall
Space Flight Center,
Huntsville, Alabama*

GROUP 4

Downgraded at 3 year intervals;
declassified after 12 years

~~CONFIDENTIAL~~

SECURITY NOTE

This document contains information affecting the national defense of the United States within the meaning of the Espionage Law, Title 18, U.S.C., Section 793 and 794, as amended. The transmission or revelation of its contents in any manner to an unauthorized person is prohibited by law.

CASE FILE COPY

~~CONFIDENTIAL~~

GEORGE C. MARSHALL SPACE FLIGHT CENTER

Technical Memorandum X-53041

April 29, 1964

RIGID BODY STUDY OF CONTROL, SEPARATION, AND
LIFT-OFF FOR SA-6 VEHICLE (U)

By

E. L. Sullivan, D. O. McNiel,
and W. H. Harmon

~~GROUP 4
Downgraded at 3 year intervals;
declassified after 12 years~~

FLIGHT MECHANICS BRANCH
AERO-ASTRODYNAMICS LABORATORY

~~CONFIDENTIAL~~

GEORGE C. MARSHALL SPACE FLIGHT CENTER

Technical Memorandum X-53041

RIGID BODY STUDY OF CONTROL, SEPARATION, AND
LIFT-OFF FOR SA-6 VEHICLE (U)

By E. L. Sullivan, D. O. McNiel,
and W. H. Harmon

13965

(U) ABSTRACT

A

This report presents a rigid body analysis of the dynamics of the control, separation, and lift-off motion of the SA-6 vehicle for the predicted standard trajectory.

A headwind restriction of 27 meters per second is imposed on the vehicle flight in order not to exceed the 5.5° angle-of-attack limitation due to structural considerations. The wind restriction is a headwind due to programmed 4° angle-of-attack in the maximum dynamic pressure region. With this wind restriction, the launch probability is still approximately in the 3σ confidence level for the four months May through August.

Under the disturbances considered in this study, there is no collision or control problem during separation of the S-I/S-IV stages for the predicted SA-6 flight.

The "close" launch support equipment is not an obstacle to the lift-off of the SA-6 vehicle under the disturbances considered. A collision problem with the umbilical tower does exist if control engine no. 1 should fail very early in flight; however, this occurrence must be considered highly improbable.

encl.

AUTHOR

(U) TABLE OF CONTENTS

	<u>Page</u>
I. INTRODUCTION.....	1
II. VEHICLE DESCRIPTION AND TRAJECTORY INFORMATION.....	2
III. ANALYSIS:	
A. Control.....	3 - 5
B. Separation.....	6 - 7
C. Lift-Off.....	8 - 9
IV. CONCLUSIONS.....	10

(U) LIST OF ILLUSTRATIONS

	<u>Title</u>	<u>Page</u>
Table	SA-6 Propelled Flight Trajectory (Stage 1).....	11
Figure		
1.	Variation of CP, CG, $C_{z_{\alpha}}$ Versus Flight Time.....	12
2.	Moment of Inertia Versus Flight Time.....	13
3.	Dynamic Pressure Versus Flight Time.....	14
4.	May and June Wind Profile Envelopes.....	15
5.	C_1 and C_2 Versus Flight Time.....	16
6.	C_1/C_2 Versus Flight Time.....	17
7.	Control Gains Versus Flight Time.....	18
8.	Angle of Attack Versus Flight Time (Bias Tilt - No Disturbance).....	19
9.	Maximum Angle of Attack Versus Flight Time.....	20
10.	Maximum Gimbal Angle Versus Flight Time.....	21
11.	Maximum Angle of Attack Versus Wind Speed ($t = 68$ sec)..	22
12.	Wind Speed Limit Versus Wind Azimuth.....	23
13.	Accumulated Attitude Error for Guidance Activation.....	24
14.	Schematic of S-I/S-IV Interstage.....	25
15.	Lateral and Longitudinal Translation of a Point on S-IV Expansion Nozzle Relative to S-I/S-IV Interstage, Subject to 3σ Disturbance.....	26
16.	Lateral and Longitudinal Translation of a Point on S-IV Expansion Nozzle Relative to S-I/S-IV Interstage, Subject to Engine Failures.....	27

(U) LIST OF ILLUSTRATIONS (Continued)

	<u>Title</u>	<u>Page</u>
Figure		
17.	Yaw Attitude Deviation as a Function of Time from Separation Signal.....	28
18.	Roll Attitude Deviation as a Function of Time from Separation Signal.....	29
19.	Vehicle Impact Points Associated with Abort Times.....	30
20.	Launch Complex VLF 37-B.....	31
21.	Drawing of SA-6 Vehicle, Showing "Close" Launch Support Equipment.....	32
22.	Lift-Off Motion of Vehicle Subject to 3σ Disturbances...	33
23.	Lift-Off Motion of Vehicle Subject to Engine Failures...	34
24.	Trace of a Point on Inboard Turbine Exhaust Duct Adjacent to Fuel Fill Mast.....	35
25.	Trace of a Point on Shroud Adjacent to Holddown Arm.....	36
26.	Trace of a Point on Shroud Adjacent to Short Cable Mast.....	37

GEORGE C. MARSHALL SPACE FLIGHT CENTER

Technical Memorandum X-53041

RIGID BODY STUDY OF CONTROL, SEPARATION, AND
LIFT-OFF FOR SA-6 VEHICLE

By E. L. Sullivan, D. O. McNiel,
and W. H. Harmon

(U) SUMMARY

This report presents a rigid body analysis of the dynamics of the control, separation, and lift-off motion of the SA-6 vehicle for the predicted standard trajectory.

A headwind restriction of 27 meters per second is imposed on the vehicle flight in order not to exceed the 5.5° angle-of-attack limitation due to structural considerations. The wind restriction is a headwind due to programmed 4° angle-of-attack in the maximum dynamic pressure region. With this wind restriction, the launch probability is still approximately in the 3σ confidence level for the four months May through August.

Under the disturbances considered in this study, there is no collision or control problem during separation of the S-I/S-IV stages for the predicted SA-6 flight.

The "close" launch support equipment is not an obstacle to the lift-off of the SA-6 vehicle under the disturbances considered. A collision problem with the umbilical tower does exist if control engine no. 1 should fail very early in flight; however, this occurrence must be considered highly improbable.

I. (U) INTRODUCTION

Rigid body control requirements are investigated for the SA-6 predicted flight. The study is conducted for the first stage flight time through separation with emphasis on the lift-off, maximum dynamic pressure, and separation times of flight. Wind restrictions are established based on structural limitations. It is also shown that there are no problems during lift-off and separation for the SA-6 vehicle. S-IV control requirements are also investigated.

The analysis for this study is presented in three sections, i.e., rigid body control, separation, and lift-off, in that order.

~~CONFIDENTIAL~~

II. (C) VEHICLE DESCRIPTION AND TRAJECTORY INFORMATION

The first stage propulsion system of the SA-6 vehicle consists of eight modified H-1 engines, rated at 188K pounds thrust per engine at sea level. The second stage (S-IV) of the SA-6 vehicle is propelled by six Pratt and Whitney engines, which develop 15K pounds each under vacuum conditions. Pertinent performance data are:

First Stage

Lift-Off Mass.....	512,906 (kg)	1,130,764 (lbm)
Thrust (Sea Level).....	6,725,364 (N)	1,511,192 (lbf)
Specific Impulse (Sea Level).....	256 (sec)	
Total Propellant (LOX/RP-1) Mass.....	385,553.6 (kg)	850,000 (lbm)
Lift-Off Acceleration.....	13 (m/sec ²)	

Second Stage

Lift-Off Mass.....	65,894.0 (kg)	145,271 (lbm)
Thrust (Vacuum).....	397,260 (N)	89,308 (lbf)
Specific Impulse (Vacuum).....	429.5 (sec)	
Total Propellants (H ₂ /O ₂) (Mass).....	45,722.1 (kg)	100,800 (lbm)

Payload

Orbital Payload (Mass).....	7,711.1 (kg)	17,000 (lbm)
-----------------------------	--------------	--------------

This study is based on the predicted, propelled flight phase of the SA-6 vehicle through separation of S-I/S-IV stages. A brief history of the first stage propelled flight is given in the Table. The powered flight is based on nominal eight-engine booster operation using a biased tilt program. The tilt program is biased to create a 4° angle of attack in the maximum dynamic pressure region under nominal conditions. This programmed angle of attack is needed in order to evaluate control forces, fin loads, and establish stability ratios more accurately than was possible on SA-5.

~~CONFIDENTIAL~~

III. (C) ANALYSIS

A. (C) Control

The histories of the motion of the center of gravity (CG) and center of pressure (CP) over flight time are shown on Figure 1. This time history of the motion of CG and CP shows the vehicle to be aerodynamically stable; i.e., the CG is forward of the CP, from approximately 47 seconds to 58 seconds of flight, when the velocity is around Mach 1. The slope of the normal force coefficient as a function of flight time is also shown on this same Figure 1. Shown on Figure 2 is the pitch moment of inertia as a function of flight time for the SA-6 vehicle. Figure 3 gives the dynamic pressure (q) over flight time for the powered phase of the booster flight.

The wind disturbances used in this analysis are based on the May and June median winds and the May and June three-sigma headwinds. These wind profiles are shown on Figure 4. The wind shears and embedded gusts used are based on the 99% confidence level. The method used in the application of the wind disturbances to the vehicle is given in Reference 1.

The aerodynamic restoring moment coefficient (C_1) and control moment coefficient (C_2) as a function of flight time are shown on Figure 5. The ratio of the aerodynamic restoring moment coefficient to control moment coefficient (C_1/C_2) is shown on Figure 6 as a function of flight time. The ratio reaches a local peak instability of $-.07$ at approximately 35 seconds, a peak positive stability of $.13$ at approximately 52 seconds, and then peak instability of $-.53$ at approximately 82 seconds.

A double sensing control system, utilizing a missile-fixed accelerometer and attitude control, is used in the pitch and yaw planes. The accelerometers are located in the instrument compartment at approximately station 1500. A second order differential equation for a mathematical simulation of the accelerometer and attitude filters is used. This simulation is good up to a frequency of approximately .6 cycles per second. The control gains (a_0, g_2) used are those furnished by R-ASTR-F (Reference 2) and are presented as a function of flight time on Figure 7.

Shown on Figure 8 is the initial angle of attack for the nominal flight trajectory, which gives a 4° angle of attack in the maximum dynamic pressure region. Angle-of-attack (α) peaks are shown on Figure 9 for the median or most probable winds for May and June and for the 3σ headwinds for May and June for the flight time of 45 to 80 seconds. This includes the maximum dynamic pressure time of flight.

CONFIDENTIAL

The band, as shown on this figure, indicates that for the 3σ headwinds, which is the most critical direction, the angle of attack is within the 5.5° limit due to structural loads. The median or most probable winds for May and June show a decrease in the angle of attack since these winds are tailwinds. The disturbances used to obtain these peaks, other than the annual winds, include the 99% probability shears and gusts, the 95% probability C_1, C_2 variations (Reference 3), and a $\pm 10\%$ variation for control gains (a_0, g_2) (Reference 2). The effects of these variations are all combined by the root sum square method. Shown also on Figure 9 is the angle-of-attack limit due to structural loads for the high dynamic pressure time point ($t = 68$ sec). Limits for other time points are not available at this time; however, the high dynamic pressure time point is normally the most critical for structural loads.

Figure 10 shows the gimbale angle (β) peaks for the same time of flight as above and with the same disturbances. Also shown on Figure 10 is the gimbale angle for the median winds without C_1 and C_2 variations.

Shown in the table below is the individual effect of the various disturbances on the angle of attack and gimbale angle for the time point of 68 sec., i.e., the maximum dynamic pressure time point. A 3σ June headwind is used to obtain these values. These effects will vary for different wind magnitudes and different times of flight, but these values are typical.

	Programed Tilt	Wind Shears	Wind Gusts	C_1, C_2 Variations	a_0, g_2 Gains
Angle of Attack	3.85	.58	1.04	.42	.12
Gimbale Angle	1.42	.43	.63	1.95	.02

Based on past history for Saturn I flights and information from R-AERO-DD, the nonrigid body effects on control of SA-6 should not exceed .2 degree in β with the angle-of-attack effect being negligible.

Figure 11 shows the angle of attack as a function of wind speed for the most critical time point ($t = 68$ sec). It is shown here that the 5.5° angle-of-attack limit for this time point gives a wind restriction of approximately 27 meters per second for a headwind, 78 meters per second for a tailwind. It has been determined that the cross-wind limit for the vehicle is 59 m/sec.

Figure 12 shows the wind speed limits as a function of wind azimuth, using the wind speed limits as given above. The launch probability for the four months May through August is 0.998, 0.998,

CONFIDENTIAL

0.987, and 1.000, respectively. These launch probability estimates are given, assuming that the maximum q wind limits will be the limiting wind speed and that the disturbances are combined statistically. Figure 12 also depicts the limits for various assumptions and combinations of disturbances upon which a decision for launch could be based. If the wind velocity is below the shaded portion of the figure, a definite "go" condition exists. If the wind velocity is within the shaded portion, a preflight simulation would be necessary to determine "go" or "no go." Wind velocities above the shaded portion are a definite "no go."

An investigation of the rigid body dynamics of S-IV stage after separation was conducted with emphasis placed on the portions of flight discussed below.

Fourteen seconds after separation command, active inertial reference is transferred from the ST-90 to the ST-124 platform. This may reflect a space reference error of approximately $.25^\circ$ for 3σ deviations. This deviation will have a negligible effect on the control of the vehicle.

At 17.6 seconds after separation command, adaptive guidance (ST-124) is activated. The attitude (ϕ_p) of the vehicle, subject to 3σ path disturbances (Reference 14) in the flight plane, is presented in Figure 13. This figure indicates the behavior of the vehicle in the transition period when the programmed tilt (cam) is replaced by the derived (polynomial) program. The angle development for the standard is due to the long tilt arrest period (30 sec) and the use of the SA-7 guidance polynomial. The 3σ maximum and minimum deviations are essentially due to a $\pm 2\%$ thrust deviation from nominal. The maximum tilt rate is 1° per second. The maximum gimbal angle requirement was found to be approximately 1° . No control problems exist.

At approximately 627.6 seconds the S-IV stage engines cut off and the vehicle becomes orbital. The attitude rate ($\dot{\phi}_p$) in the flight plane, with the thrust decay subject to 3σ disturbances, was found to be approximately .25 degrees per second, causing no control problems.

~~CONFIDENTIAL~~

B. (U) Separation

This study is divided into two phases. The first of these is an investigation of the probability of physical collision during separation "collision phase." The second part is a study of attitude (ϕ) deviations of the S-IV stage immediately following separation "control phase."

Vehicle motion for the rigid body analysis of the dynamics of separation of the S-I and S-IV stages of the SA-6 vehicle was computed using a six-degrees-of-freedom flight simulation program in which a first order mathematical simulation of the attitude (ϕ) filter is used. The sequence of events previous to and following separation for SA-6 is identical to SA-5 as outlined in Reference 4 and is briefly summarized by the following:

Time (sec)

- 6.4	Signal for S-I Inboard Cut-Off
- .4	Signal for S-I Outboard Cut-Off
- .11	Signal to Ignite Ullage Rockets
0	Separation Command (Explosive Nuts Actuate)
+ .05	Retrorocket Thrust Buildup to 10%
+ 1.7	Signal to Ignite S-IV Engines

Hardware limitations exist due to the (ST-90) inertial platform, which prohibits (ϕ) deviations in excess of -15° to $+165^\circ$ in pitch, $\pm 15^\circ$ in yaw, and $\pm 15^\circ$ in roll. If these limitations are exceeded, the platform loses its space-fixed reference. Dynamics of the vehicle are investigated, subject to the following disturbances: 3σ engine misalignments, 3σ thrust variations, 3σ wind and engine failures (note: engine failure cases in this memorandum are defined as engines that fail to ignite). These 3σ variations for thrust, misalignment, and wind are based on References 5 through 12. All disturbances are directed to produce the maximum deviation of the vehicle from nominal operation. Results obtained from the 3σ disturbances are treated in a statistical manner, whereas engine failures, due to a lack of sufficient data, are treated separately. Initial conditions were based on the SA-6 Predicted Standard Trajectory. The 3σ engine misalignments listed below are total thrust values; i.e., the total thrust vector is misaligned the stated amount.

3σ	S-I Booster (4 engines)	=	$.75^\circ$
3σ	Ullage Rocket	=	$.35^\circ$
3σ	Retrorocket	=	$.10^\circ$
3σ	S-IV Engines	=	$.60^\circ$

Phase I "Collision"

A simplified drawing, which indicates the location of the S-I/S-IV interstage in relation to the S-IV mainstage engines, is presented in Figure 14. These engines are assumed to be gimballed to and locked in the hard outboard position, leaving a minimum lateral clearance of 74 cm. Results are presented in the form of lateral and longitudinal motion of a point on the S-IV engine expansion nozzle relative to the S-I/S-IV interstage at the separation plane. Relative motion due to the following disturbances is presented in Figure 15: 3σ thrust variation (combined effect of S-I, Retro, and Ullage Thrust Variations), 3σ engine misalignment (combined effect of S-I, Retro, and Ullage Engine Misalignments), 3σ wind, and the total "combined effect." The 3σ "Total Combination" utilizes 20% of the clearance available. Results of individual engine failures are presented in Figure 16.

Phase II "Control"

Results of the control phase of this study are shown in Figures 17 and 18. These figures present attitude (ϕ) deviations in roll and the yaw plane as a function of time (time measured from the separation signal). Yaw attitude (ϕ_y) deviations due to the following disturbances are indicated in Figure 17: ullage rocket #4 failure, S-IV engine #5 failure, and a 3σ "Total Combination" (combined effect of S-I, S-IV, and ullage 3σ thrust variations, 3σ engine misalignment, and a 3σ wind). The failure of ullage rocket #4 produces the largest attitude angle ($\phi_y = 4.5^\circ$). Attitude deviations in roll are presented in Figure 18 for 3σ thrust misalignments for the mainstage S-IV engines and the ullage rockets. The latter case produced the maximum roll angle ($\phi_r = 5.7^\circ$), which is well within the $\pm 15^\circ$ limitation of the ST-90 inertial platform.

C. (U) Lift-Off

The lift-off motion of the SA-6 vehicle is described in this section. Launch is to be from AMR, launch complex VLF 37-B. Vehicle motion was computed using a six-degrees-of-freedom flight simulation program in which the earth is treated as a rotating ellipsoid. The following disturbances were considered: S-I stage engine misalignment, wind, gyro platform misalignment, and booster engine failures. Aerodynamic (Reference 13) and wind data are provided by R-AERO-A and R-AERO-Y, respectively. Nominal booster operation is assumed in this study unless indicated otherwise. The "3-sigma" engine and platform misalignments used in this study are based on alignment tolerances as outlined in Reference 6. Individual disturbances are combined by root-sum-squaring the effect of each.

The location of the launch pad with respect to the shoreline is shown in Figure 19. This figure indicates vehicle impact points associated with several abort (eight booster engine shutdown) times. It may be seen that for an abort time equal to or greater than 27 seconds the vehicle will impact in the Atlantic Ocean.

A schematic of launch complex VLF 37-B, indicating the location of the umbilical tower with respect to the SA-6 vehicle, is presented in Figure 20. As indicated in this figure, the critical structural member of the booster for tower collision is the tip of fin no. 2. The "close" launch support equipment (Figure 21), located in the proximity of the vehicle during lift-off is holddown arms, short cable masts, and propellant fill masts. In this study all disturbances are directed to produce the maximum horizontal drift of the vehicle toward the object being considered. For example, when considering the motion of the vehicle due to the effect of wind, engine misalignment or platform misalignment with respect to the umbilical tower, each disturbance is directed along a line that is 51° E of N (Figure 22). A failure of control engine no. 1 is the most critical with regard to a possible tower collision and produces a drift that is 45° E of N (Figure 23).

In this study a 3σ engine misalignment of $.53^\circ$ means that the thrust vectors of all eight booster engines are misaligned the stated amount from their canted position. Horizontal motion due to 3σ platform misalignment of $.2^\circ$, 3σ surface wind (May), 3σ engine misalignment of $.53^\circ$, and a 3σ combination of wind, platform misalignment, and engine misalignment is presented in Figure 24. Upon clearing the tower vertically, the vehicle has drifted .5, 1.3, 1.9, and 2.3 meters, respectively. No collision problem exists.

Drift, as a function of vertical displacement for no. 1 engine failures at 0, 1, 2, and 3 seconds of flight time, is presented in Figure 23. It is shown that a failure of this control engine prior to .7 seconds will present a collision problem with the tower. However, the estimated probability of a specific engine failure occurring within a specified time period of 1 second is 3×10^{-5} .

There are eight holddown arms, two propellant fill masts, and two short cable masts in the vicinity of the vehicle at lift-off. Three representative cases are presented in this memorandum, one of each of the above named "close" objects. Vehicle motion is presented in centimeters for 3σ disturbances and no. 1 engine failure (flight time = 0 sec) of a point on inboard turbine exhaust duct adjacent to fuel fill mast, shroud adjacent to holddown arm, shroud adjacent to short cable mast, in Figures 24, 25, and 26, respectively. Due to the negligible amount of drift incurred in the short period of time necessary for the vehicle to clear these "close" objects, individual wind cases are not included in these figures.

IV. (U) CONCLUSIONS

The wind restrictions for the launch of SA-6 are shown on Figures 11 and 12. Using these wind restrictions of 27 m/sec headwind, 78 m/sec tailwind, and 59 m/sec crosswind, and the predicted winds for the four months May through August, the launch probability for the SA-6 vehicle is near the 3σ confidence level for this period. This is based on the assumption that the 5.5° angle-of-attack limit for the maximum dynamic pressure time is the limiting time point for structural loads.

In the separation phase of the SA-6 vehicle flight, there is no collision or control problem under the influence of the 3σ disturbances considered here.

The close launch support equipment, i.e., holddown arms, short cable masts, and propellant fill masts, is not an obstacle to the lift-off of the SA-6 vehicle under the influence of the 3σ disturbances considered here. A collision problem with the umbilical tower does exist if control engine no. 1 should fail very early in flight; however, this occurrence must be considered highly improbable.

~~CONFIDENTIAL~~

(C) TABLE

SA-6 PROPELLED FLIGHT TRAJECTORY (STAGE 1)

8 X 188K Engines F = 1,511,192 (lbf)
850,000 (lbm) Prop. Consumption Isp = 256 (sec)

$W_o = 1,130,764$ (lbm)
 $W_c = 276,563$ (lbm)

Time (sec)	Ground Distance (km)	Altitude (km)	Velocity (m/sec)	Path Angle (deg)	Acceleration	Mach
					V Dot (m/sec ²)	
0	0	.03	0	0	0	0
20	.01	.82	84.7	.92	5.09	.25
40	.54	3.61	210.2	20.26	7.83	.63
60	3.34	8.81	383.5	33.64	8.76	1.23
65	4.50	10.47	429.4	35.78	9.68	1.41
70	5.86	12.30	481.3	37.45	11.17	1.63
75	7.43	14.30	541.9	38.93	13.11	1.88
80	9.27	16.52	612.7	40.72	15.23	2.15
100	20.49	27.72	1,008.9	49.13	24.50	3.35
120	41.11	42.96	1,602.9	57.17	35.40	4.87
140.1	75.92	62.65	2,467.7	63.37	52.42	7.91
146.1	89.54	69.36	2,628.1	64.50	26.02	8.99

Time (sec)	Mass (kg)	Dynamic Pressure (N/m ²)	Thrust (N)	Drag (N)
0	512,906	0	6,725,364	44,130
20	459,006	3,935	6,956,169	125,798
40	404,784	18,377	7,184,287	305,813
60	350,561	35,478	7,444,928	1,518,036
65	336,965	36,888	7,503,649	1,558,884
70	323,369	37,139	7,559,184	1,417,939
75	309,776	35,730	7,608,572	1,180,415
80	296,182	32,276	7,646,902	939,880
100	242,139	13,341	7,721,581	249,968
120	188,152	3,446	7,701,629	47,009
140.1	134,209	794	7,626,205	7,809
146.1	125,447	382	3,785,393	3,424

~~CONFIDENTIAL~~

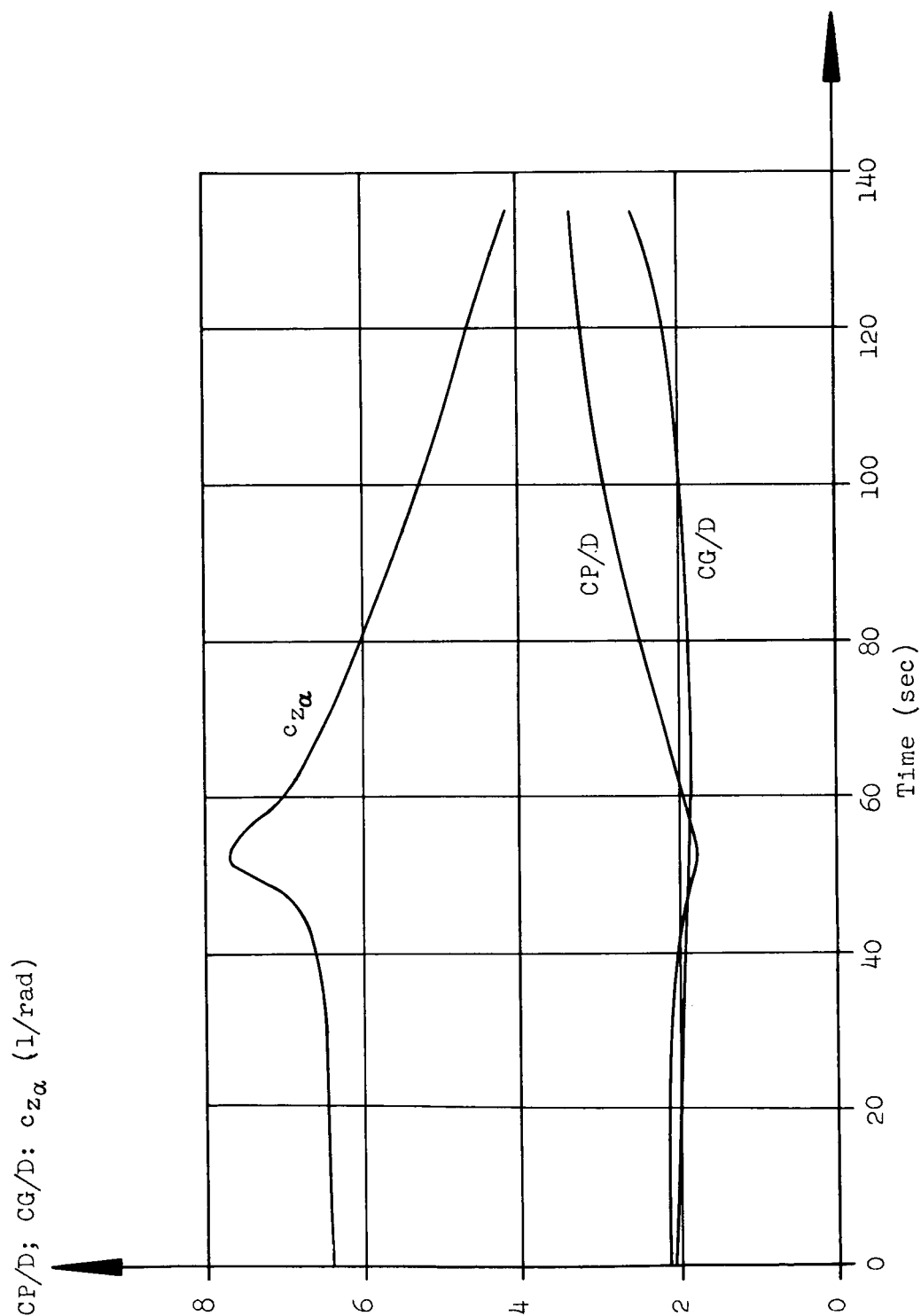
~~CONFIDENTIAL~~

FIG. 1. VARIATION OF CENTER OF PRESSURE (CP/D), CENTER OF GRAVITY (CG/D) AND SLOPE OF LIFT COEFFICIENT ($c_{z\alpha}$) WITH FLIGHT TIME.

~~CONFIDENTIAL~~

~~CONFIDENTIAL~~

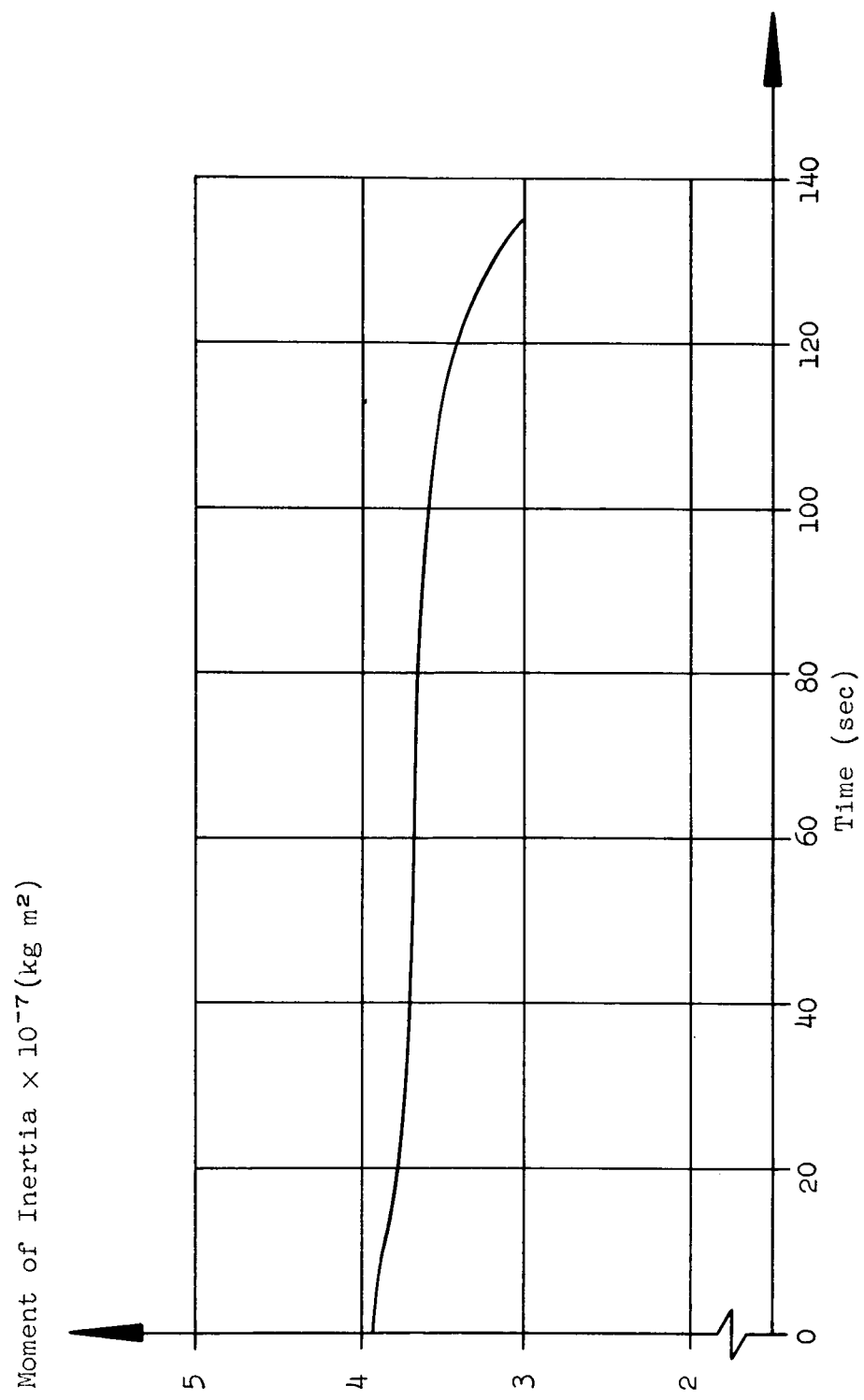


FIG. 2. MASS MOMENT OF INERTIA IN PITCH VERSUS FLIGHT TIME

~~CONFIDENTIAL~~

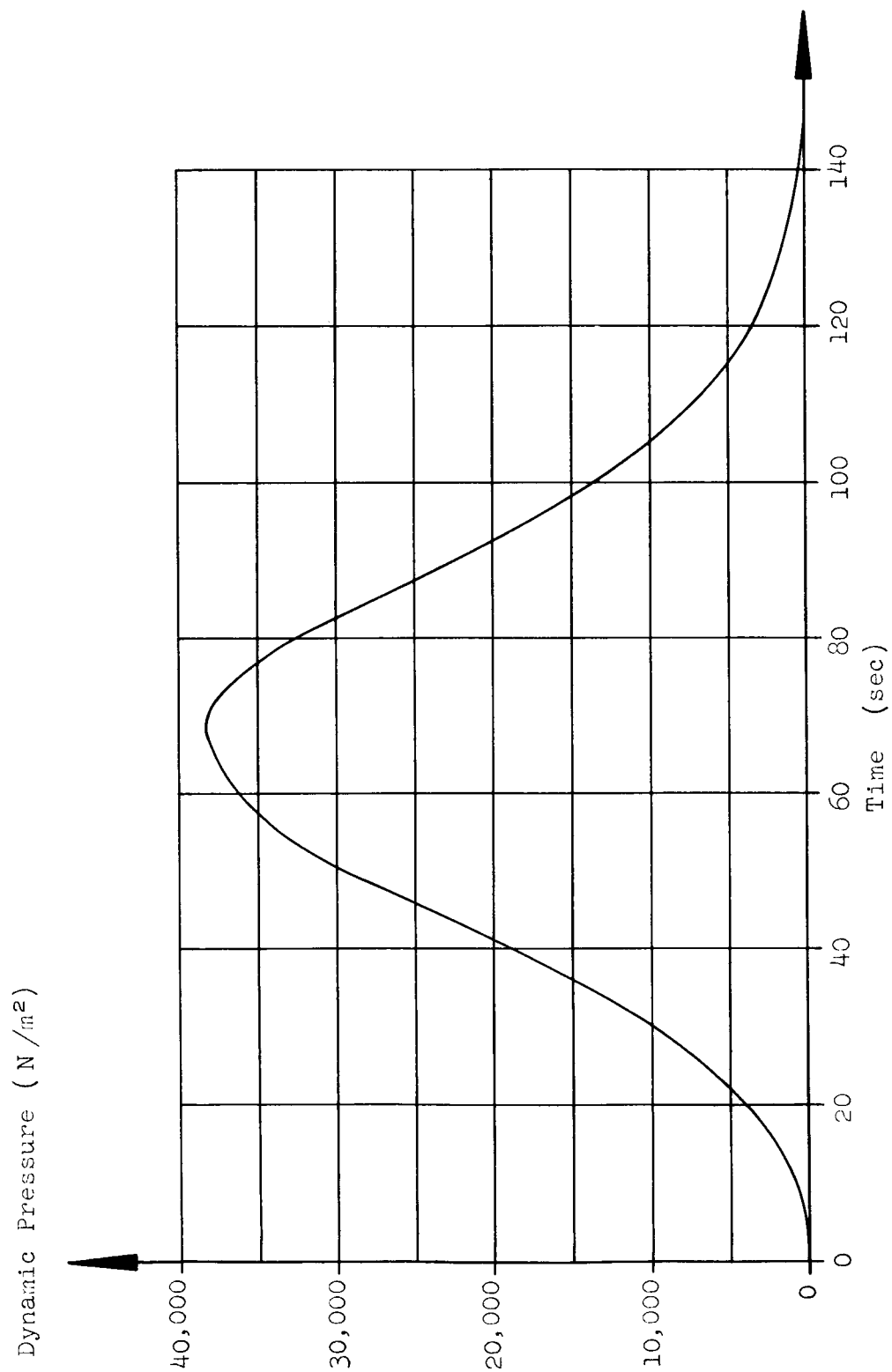
~~CONFIDENTIAL~~

FIG. 3. DYNAMIC PRESSURE VERSUS FLIGHT TIME

~~CONFIDENTIAL~~

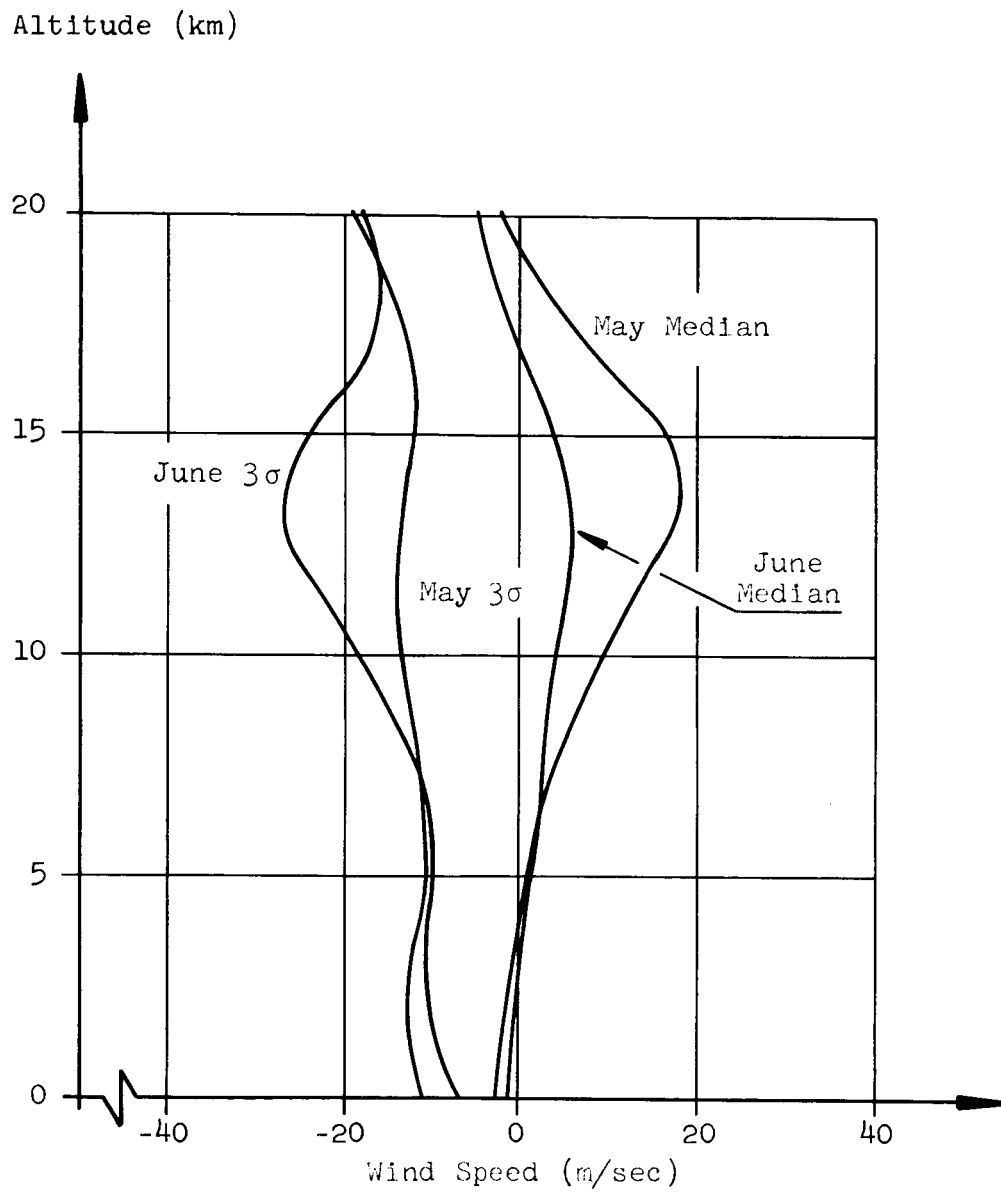


FIG. 4. WIND PROFILE ENVELOPES FOR MAY AND JUNE
(105° Azimuth; Positive Values Tailwind; Negative Values Headwind)

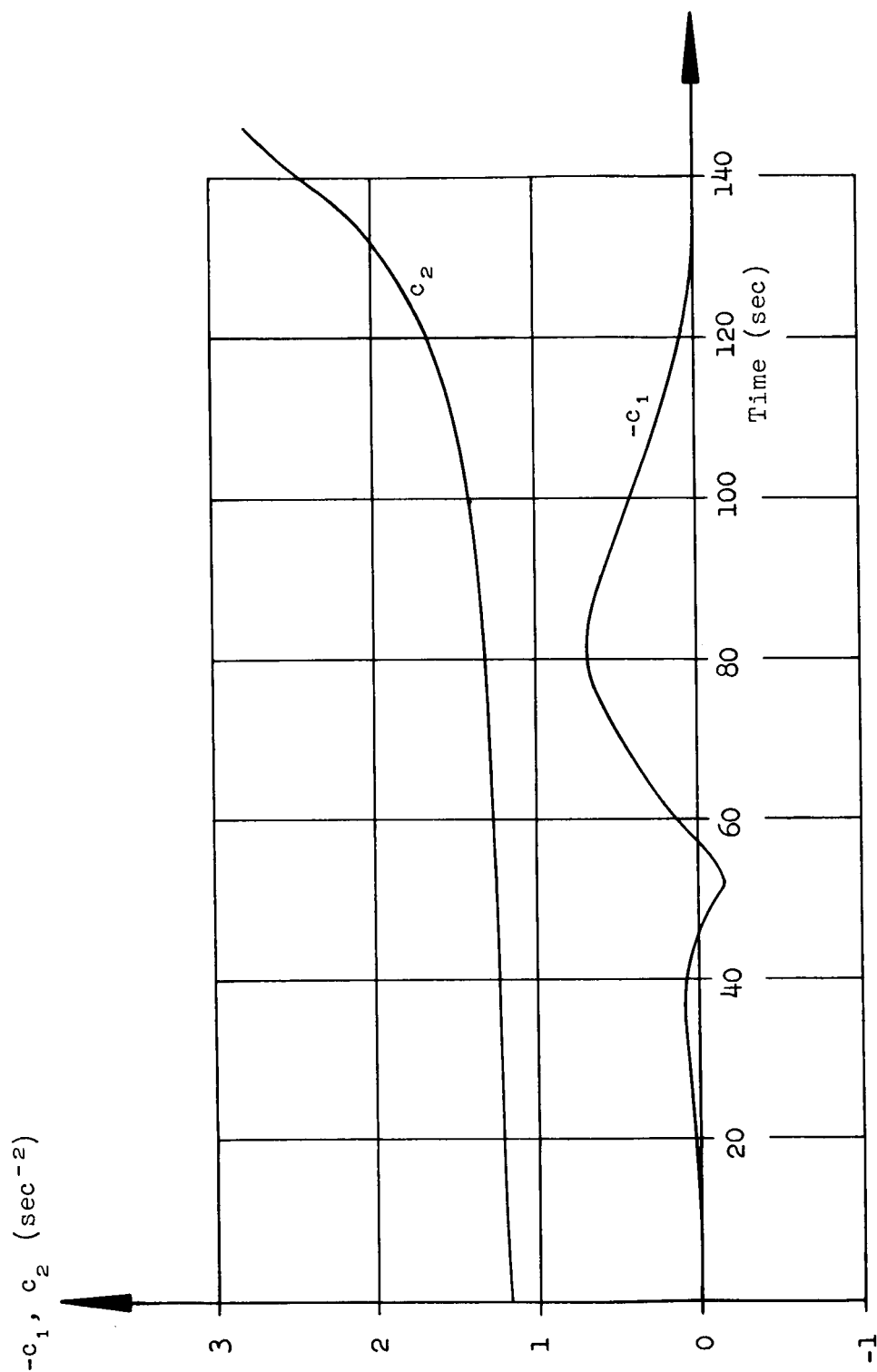


FIG. 5. AERODYNAMIC RESTORING MOMENT COEFFICIENT (c_1) AND CONTROL MOMENT COEFFICIENT (c_2) VERSUS FLIGHT TIME

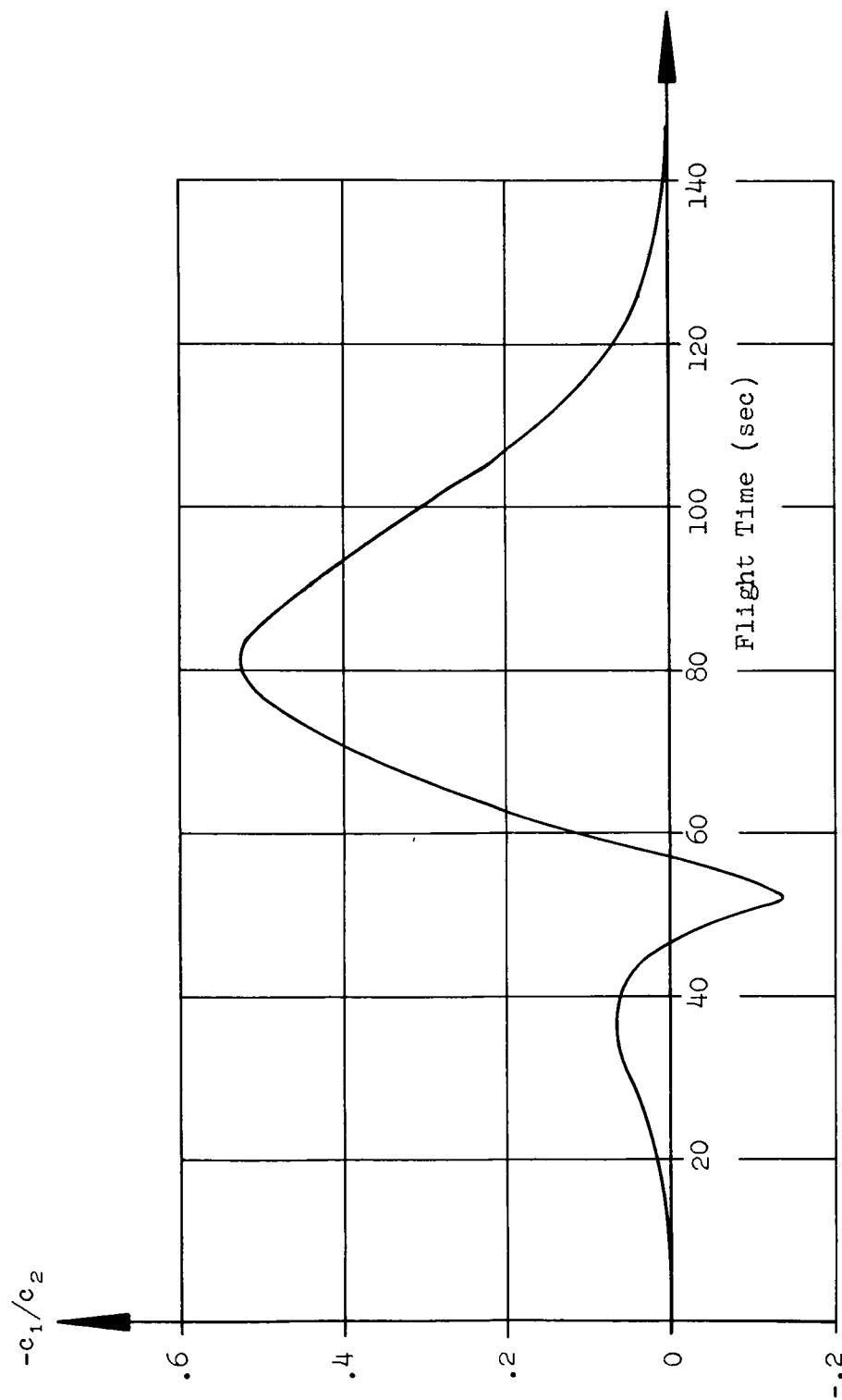


FIG. 6. RATIO OF AERODYNAMIC RESTORING MOMENT COEFFICIENT (c_1) TO CONTROL MOMENT COEFFICIENT (c_2) VERSUS FLIGHT TIME

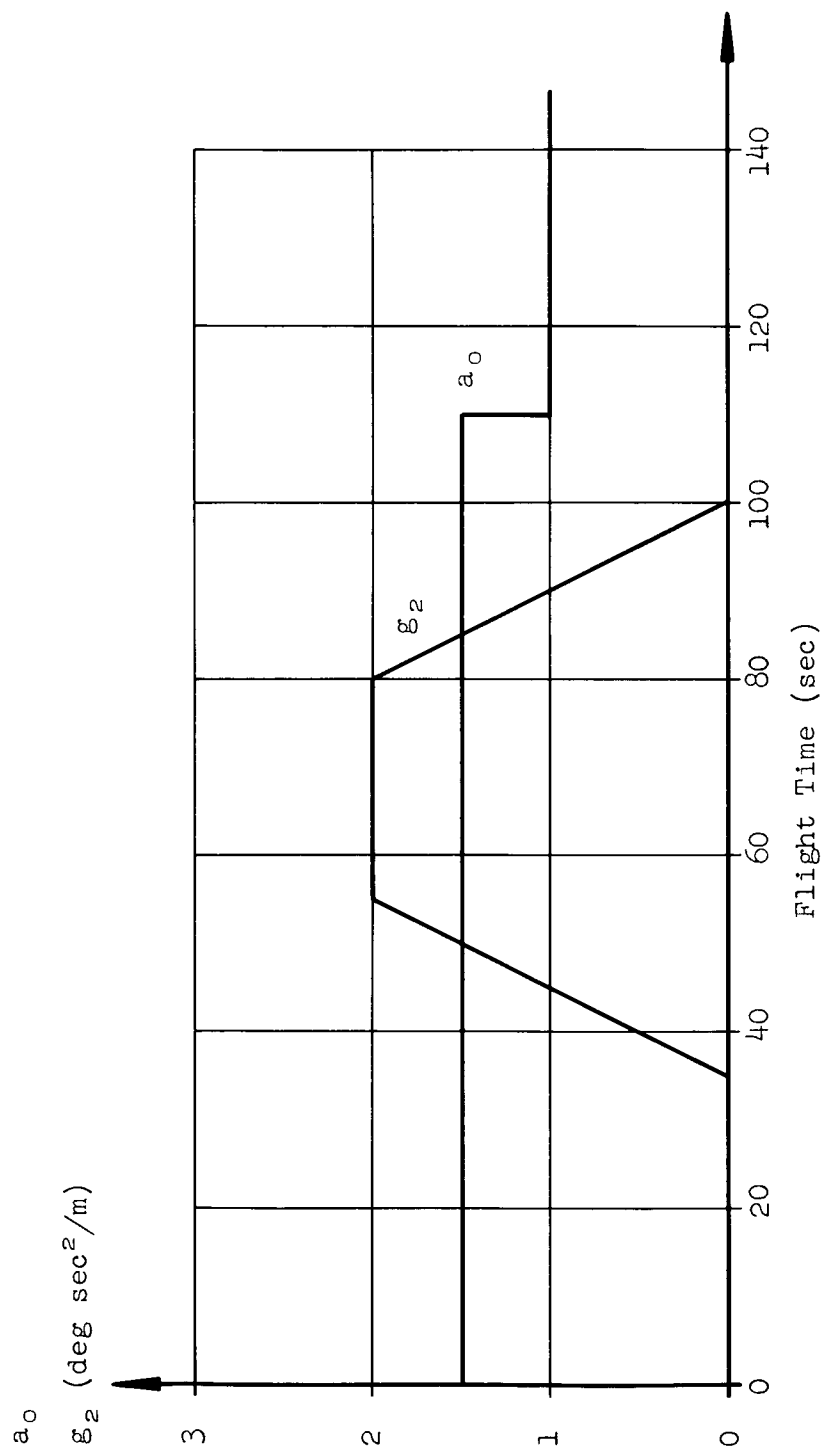


FIG. 7. CONTROL GAINS VERSUS FLIGHT TIME

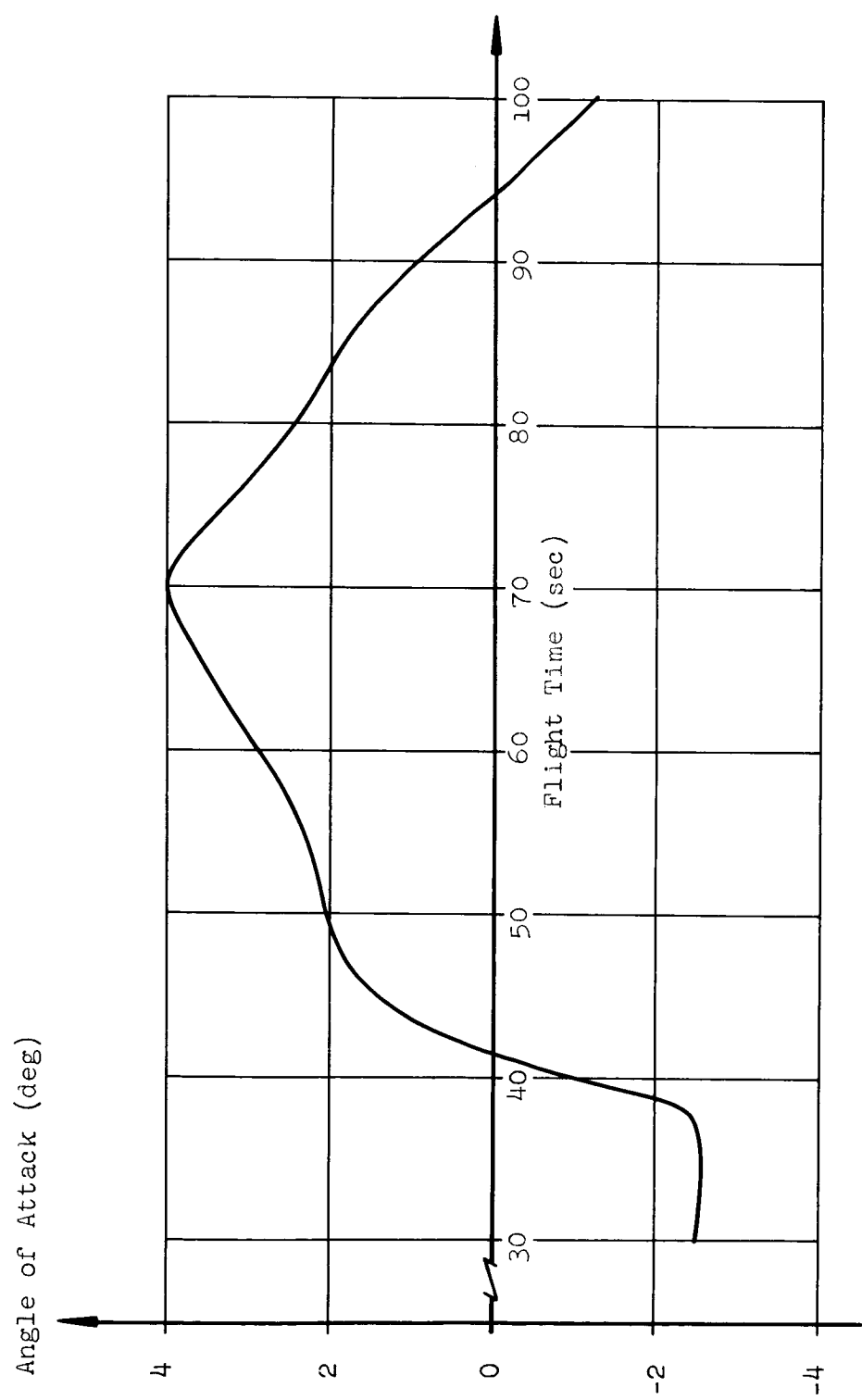


FIG. 8. ANGLE OF ATTACK VERSUS FLIGHT TIME
FOR PROGRAMMED TILT WITH NO DISTURBANCES

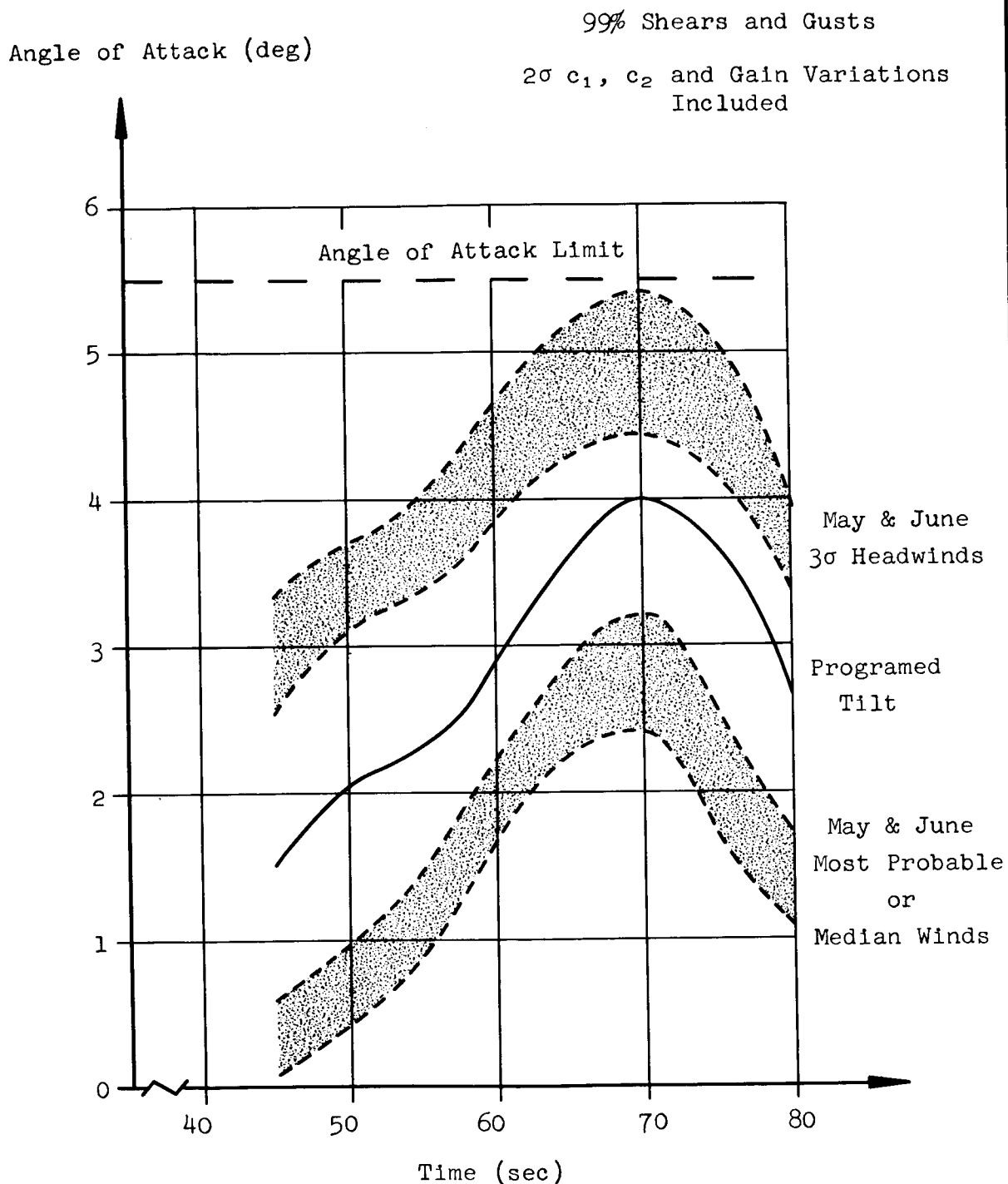
~~CONFIDENTIAL~~

FIG. 9. ANGLE OF ATTACK VERSUS FLIGHT TIME

~~CONFIDENTIAL~~

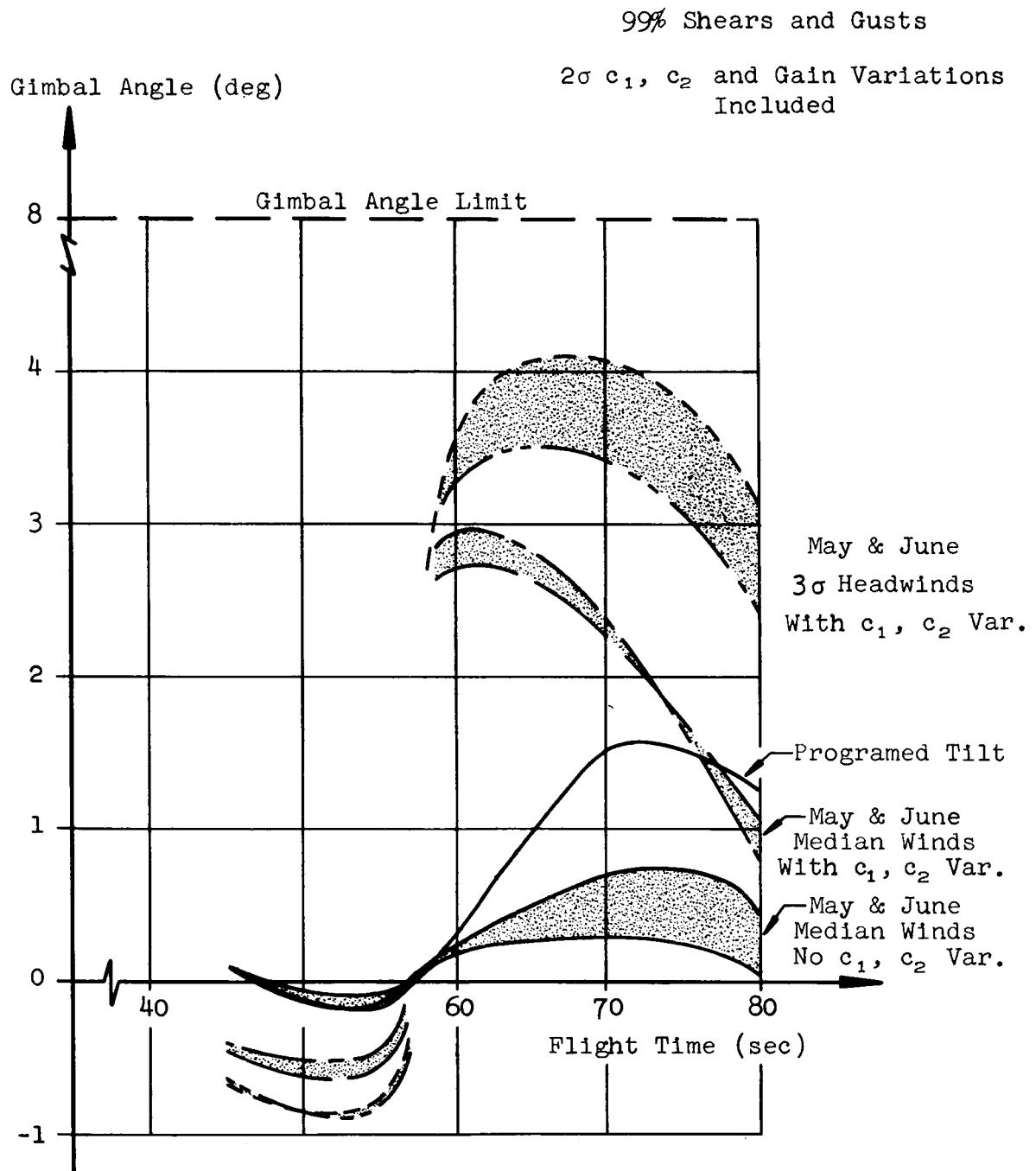


FIG. 10. GIMBAL ANGLES VERSUS FLIGHT TIME

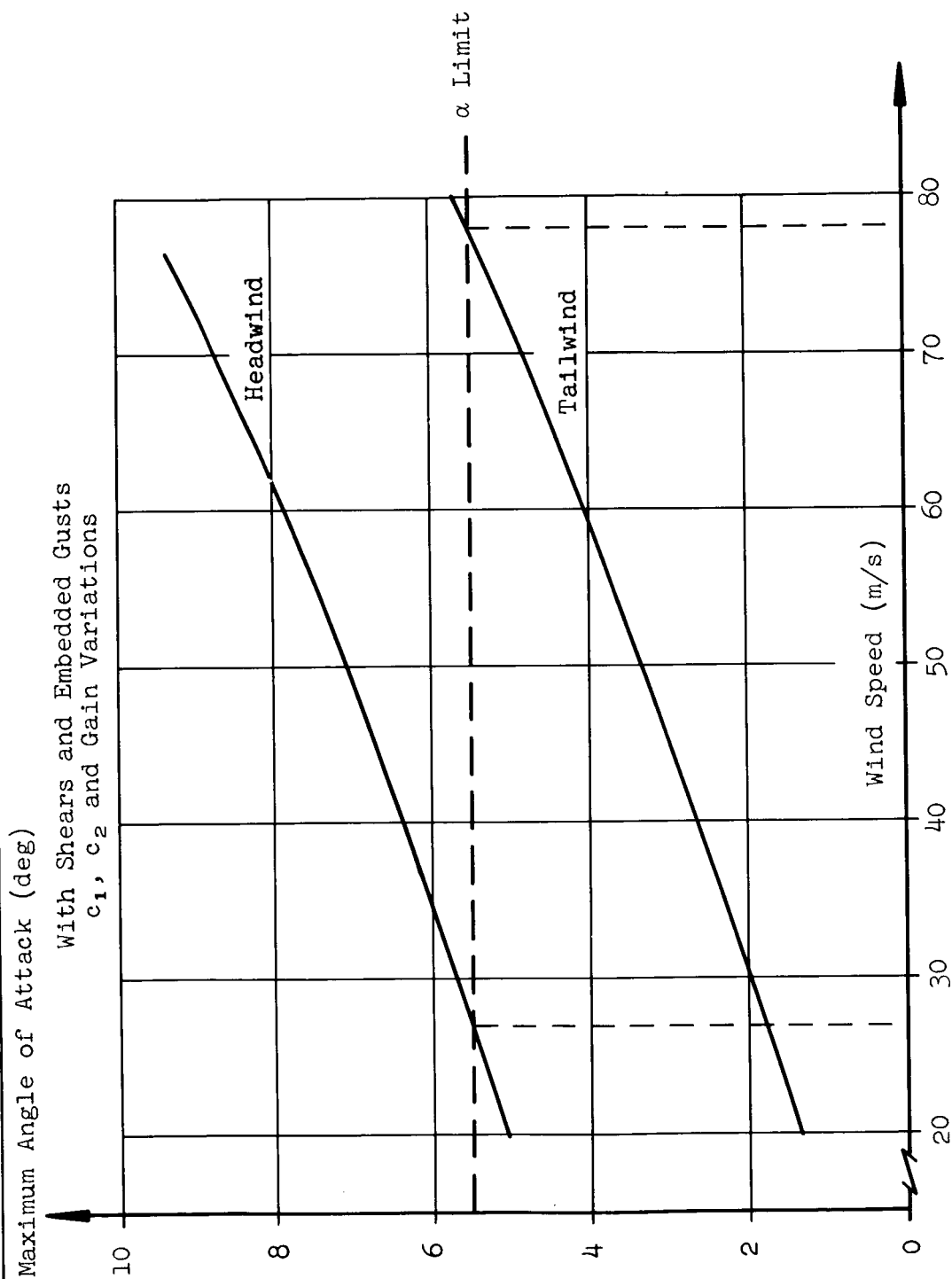


FIG. 11. MAXIMUM ANGLE OF ATTACK VERSUS WIND SPEED
FOR MAXIMUM DYNAMIC PRESSURE TIME POINT ($t = 68$ sec)

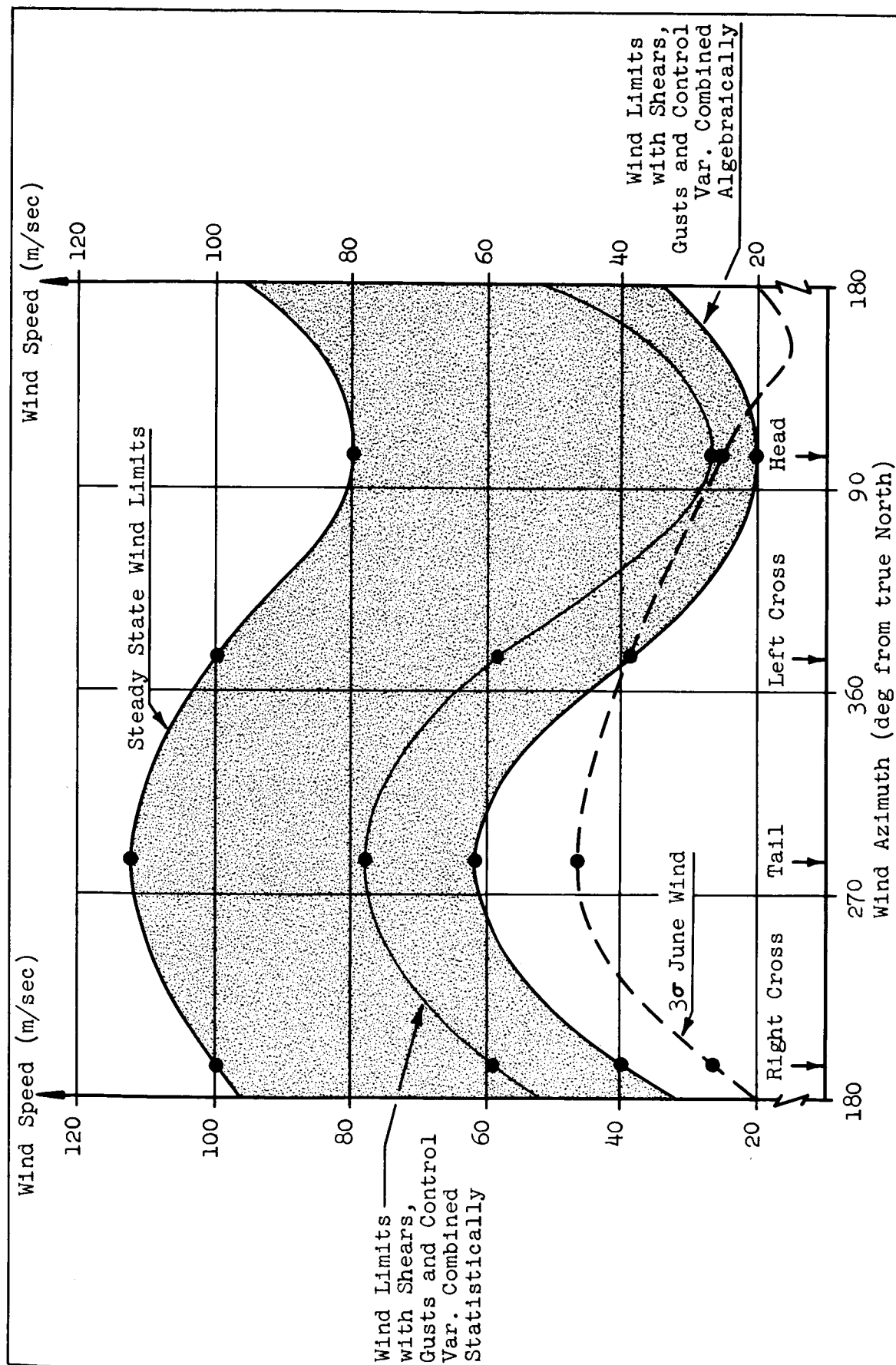


FIG. 12. SA-6 APPROXIMATE WIND SPEED LIMITS VERSUS WIND AZIMUTH
FOR MAXIMUM DYNAMIC PRESSURE TIME POINT

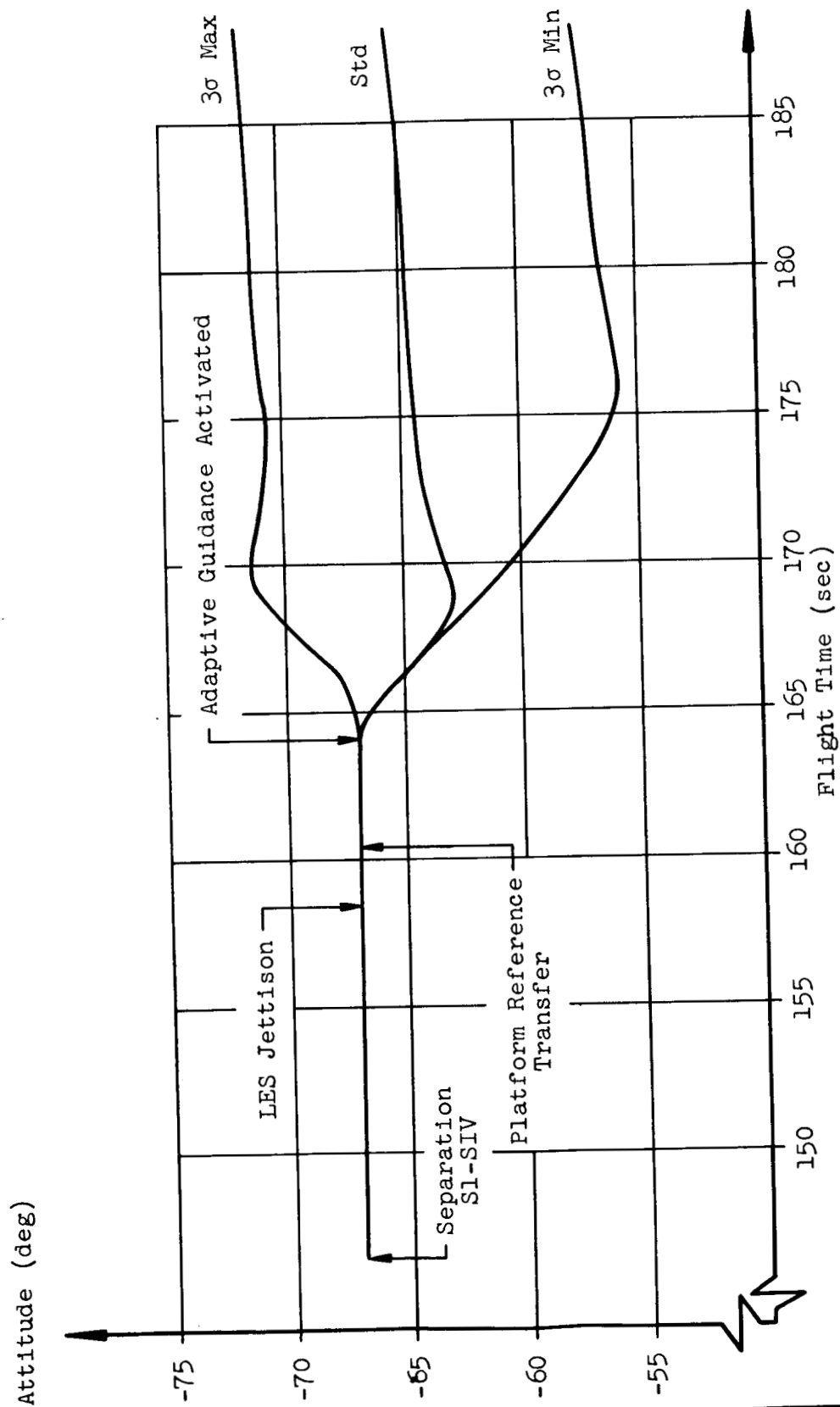


FIG. 13. ACCUMULATED ATTITUDE (ϕ_p) ERRORS FOR ST-124 ACTIVATION

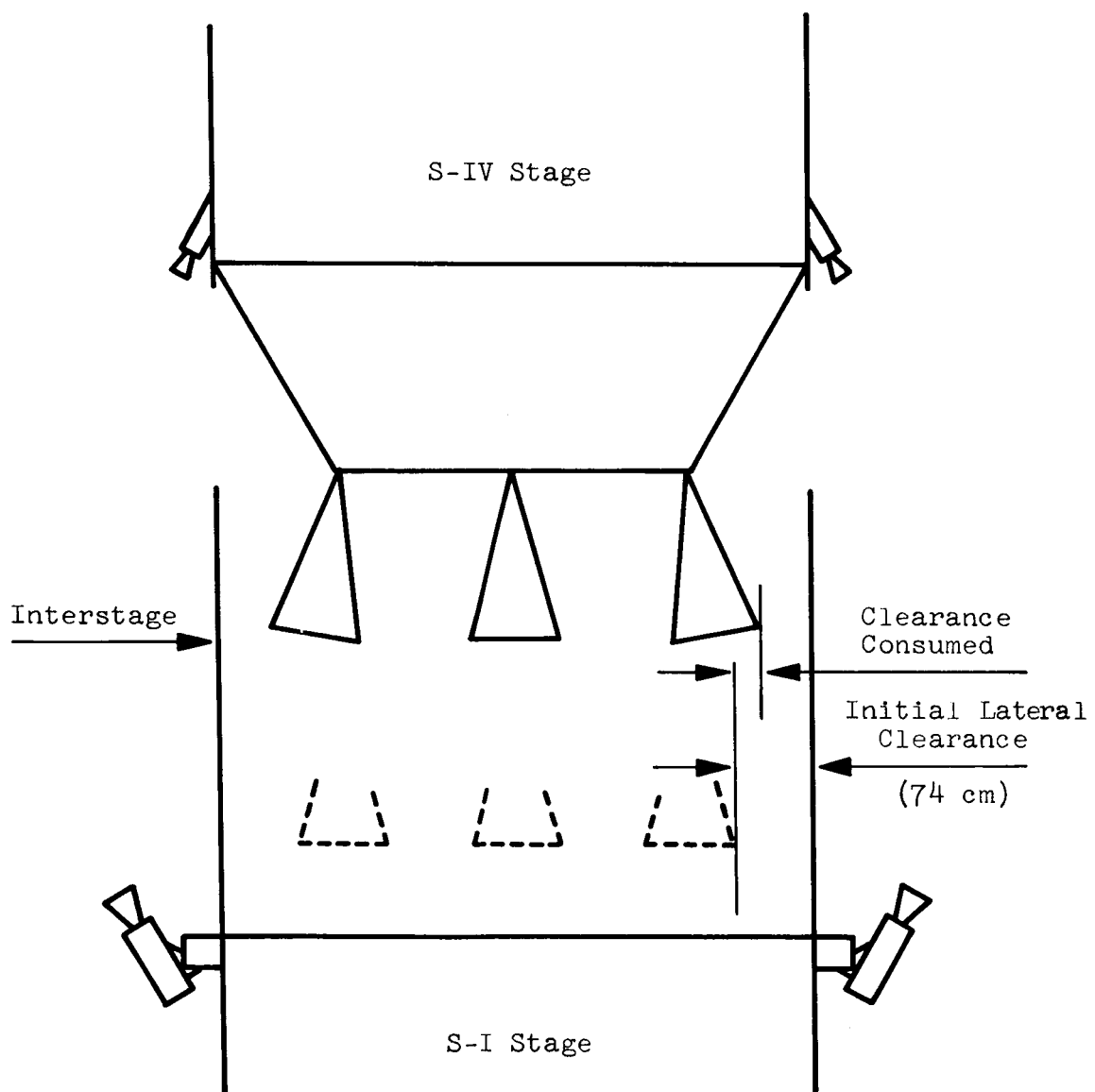


FIG. 14. SCHEMATIC OF S-I/S-IV INTERSTAGE

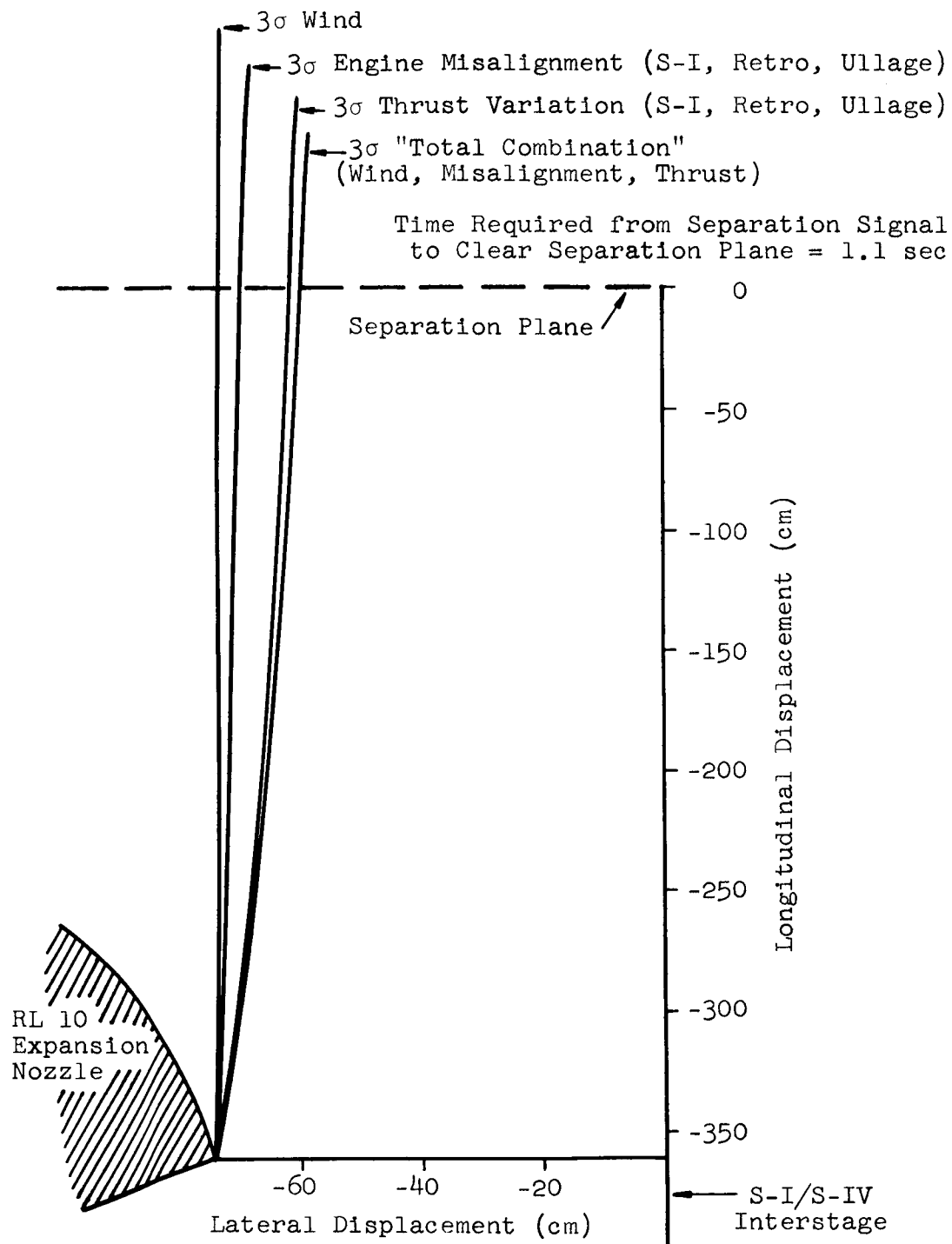


FIG. 15. LATERAL AND LONGITUDINAL TRANSLATION OF
A POINT ON S-IV ENGINE EXPANSION NOZZLE
RELATIVE TO S-I/S-IV INTERSTAGE

t = Time Required from Separation Signal to Clear Separation Plane

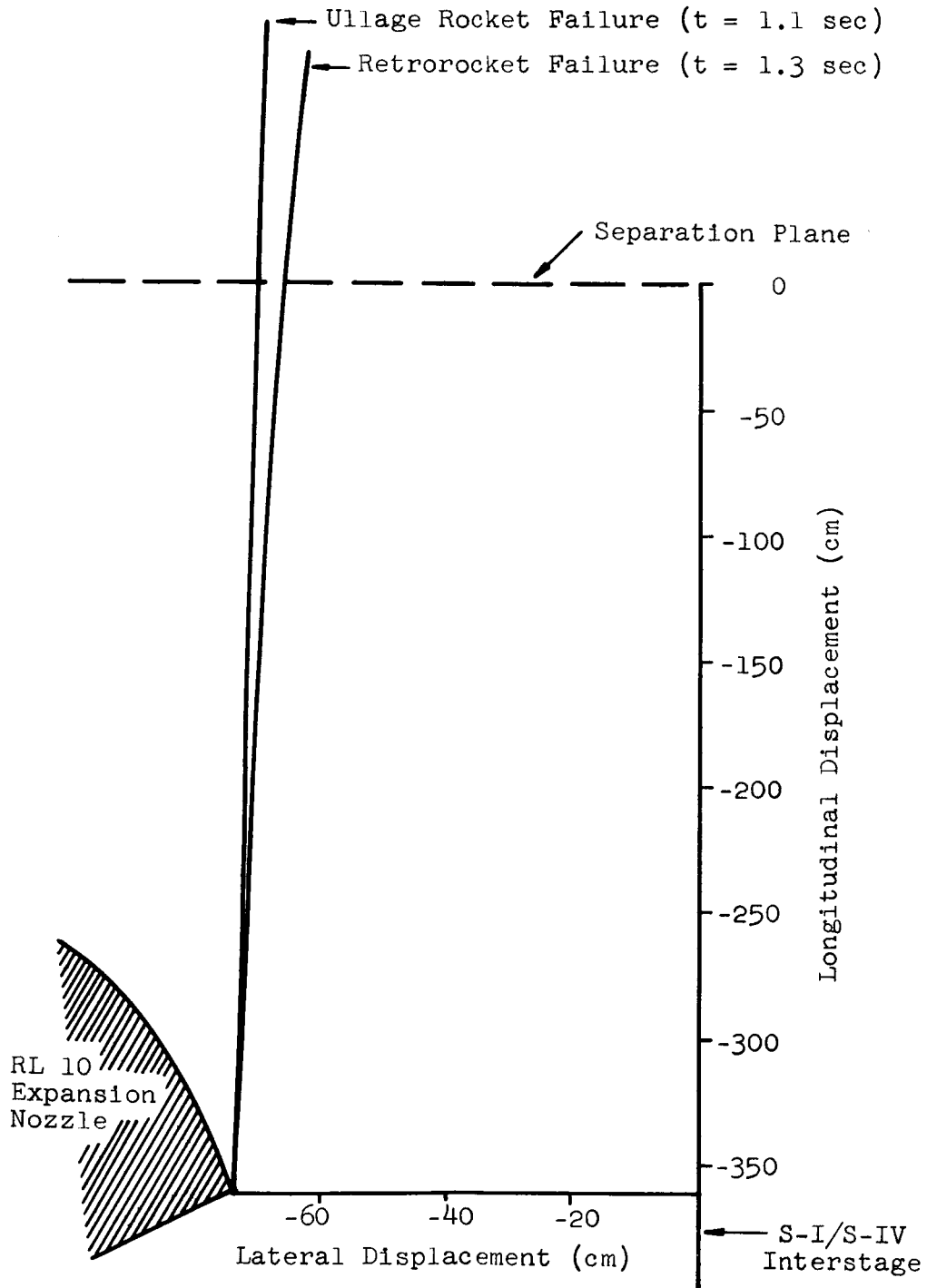


FIG.16. LATERAL AND LONGITUDINAL TRANSLATION OF
A POINT ON S-IV ENGINE EXPANSION NOZZLE
RELATIVE TO S-I/S-IV INTERSTAGE

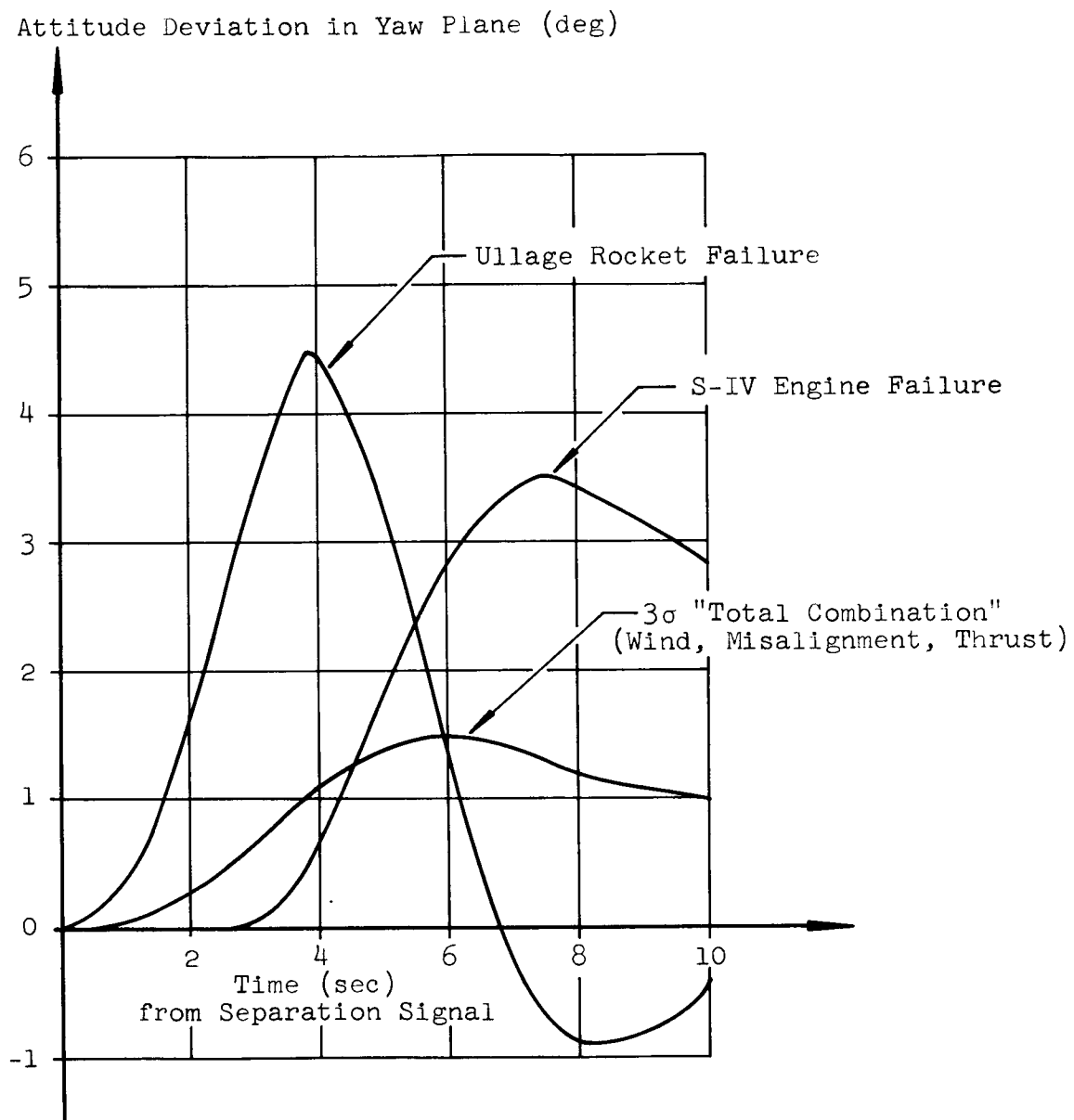


FIG. 17. YAW ATTITUDE DEVIATION
AS A FUNCTION OF TIME FROM SEPARATION SIGNAL

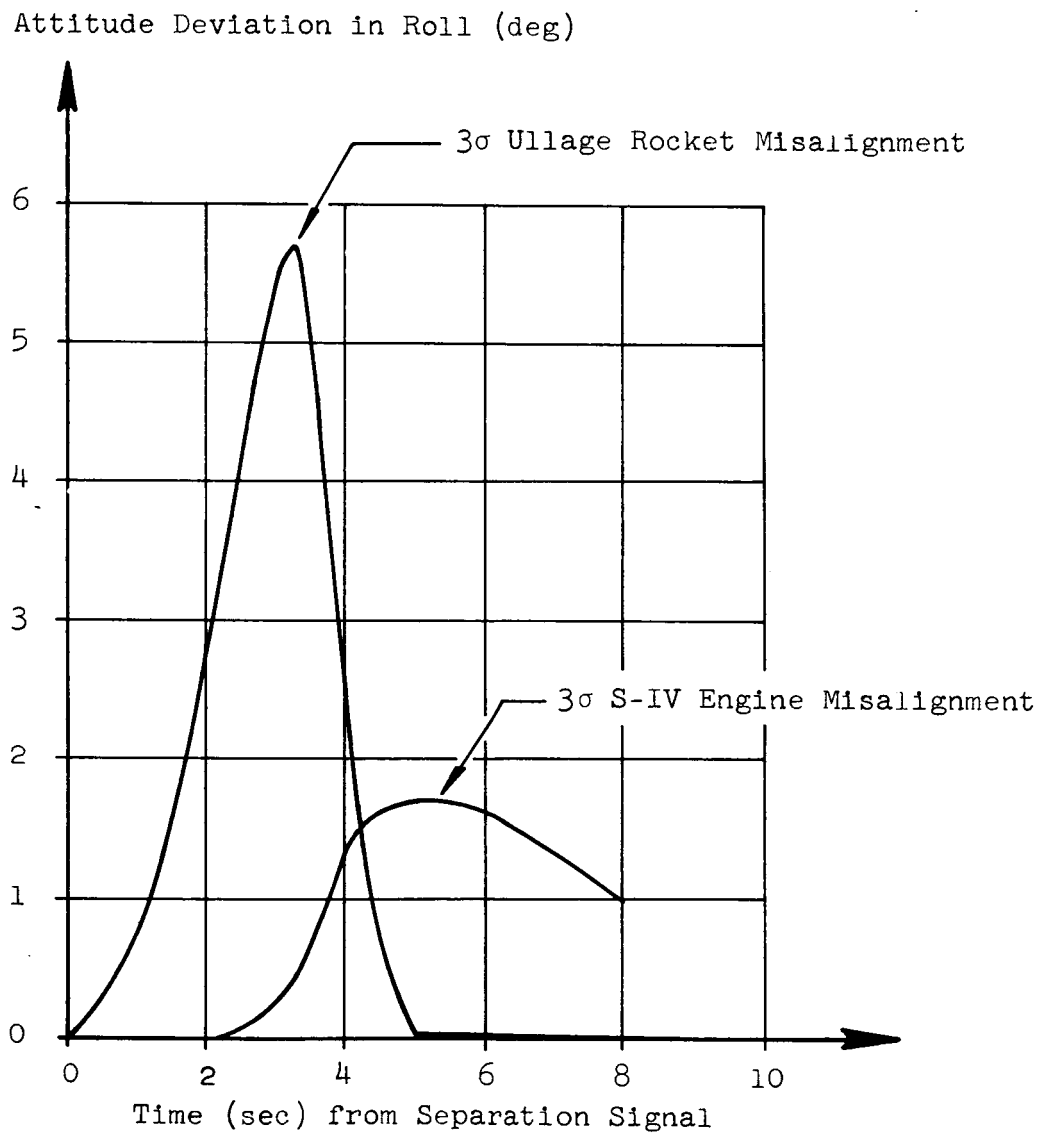


FIG. 18. ROLL ATTITUDE DEVIATION
AS A FUNCTION OF TIME FROM SEPARATION SIGNAL

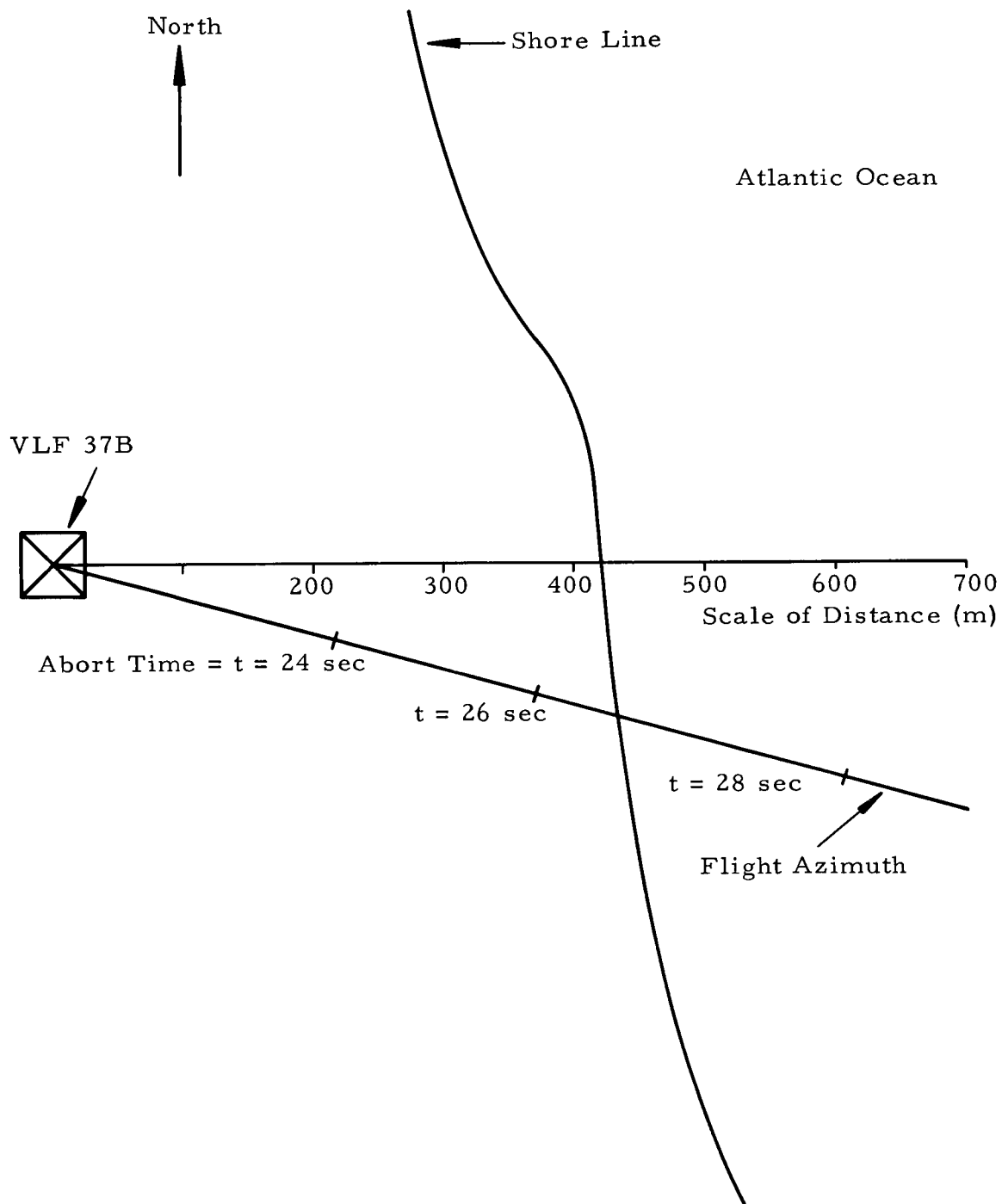


FIG. 19. GRAPH INDICATING VEHICLE IMPACT POINTS ASSOCIATED WITH ABORT (EIGHT BOOSTER ENGINE SHUT DOWN) TIMES

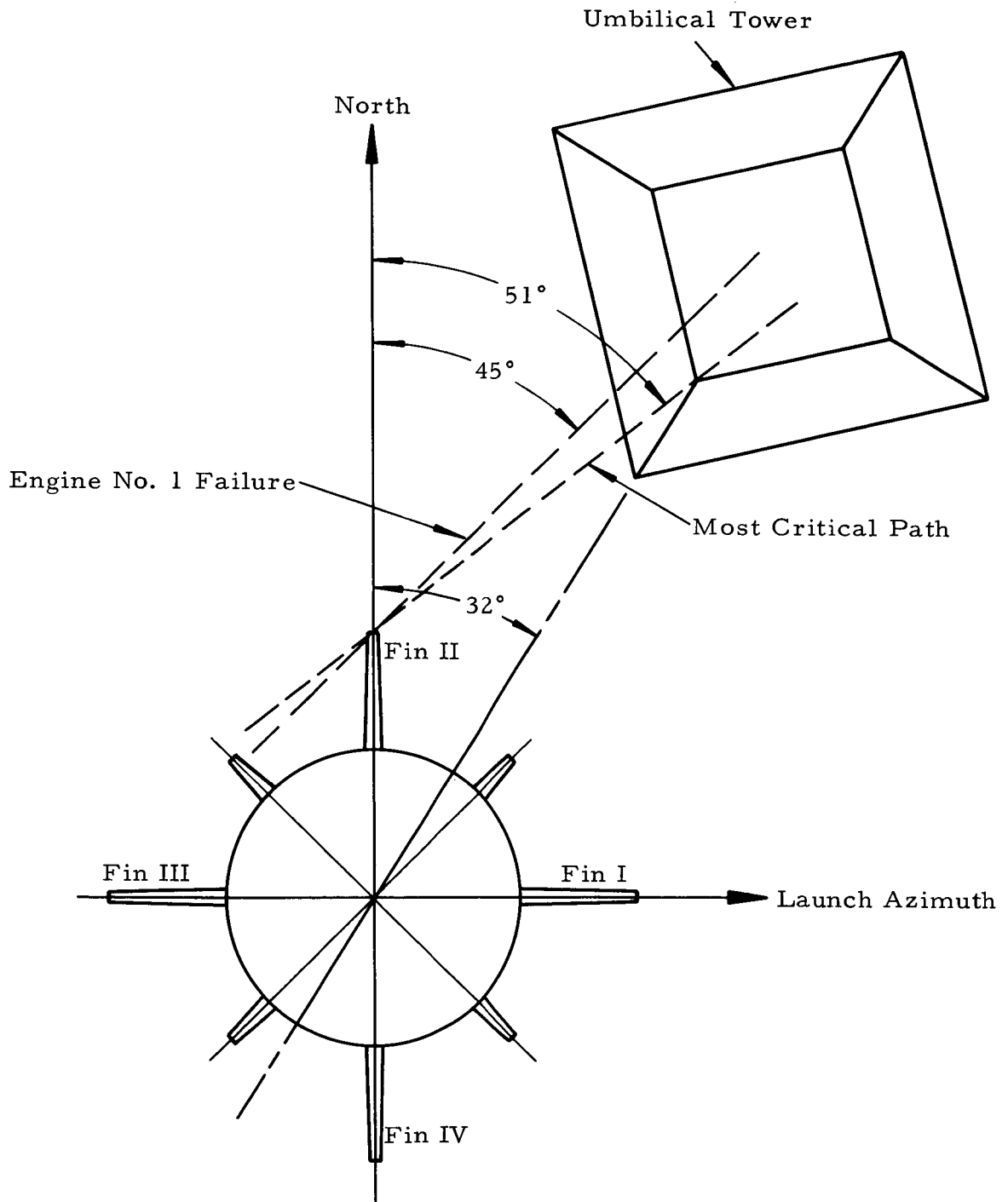


FIG. 20. LAUNCH COMPLEX VLF 37 B

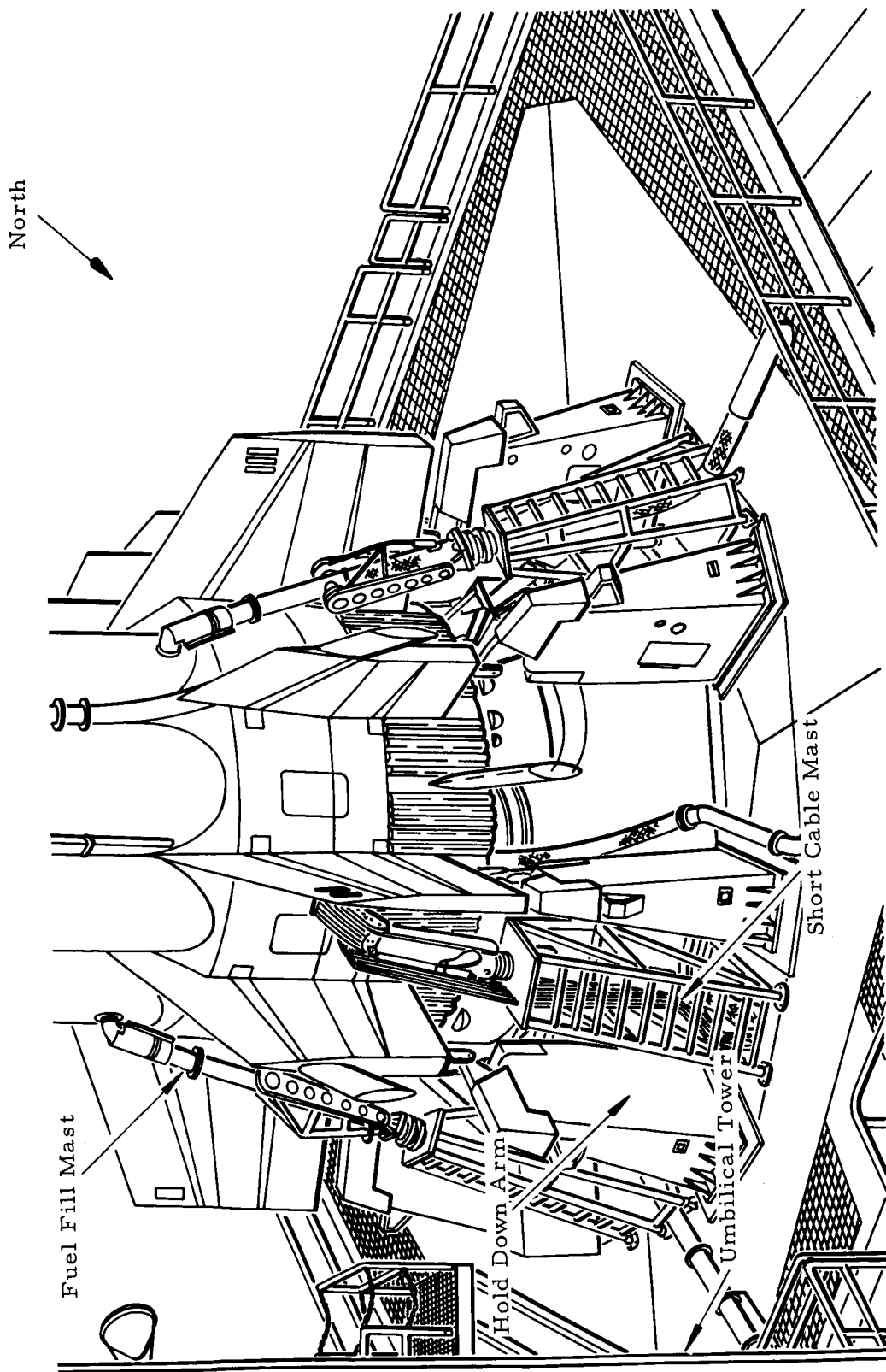


FIG. 21. DRAWING OF SA-6 VEHICLE SHOWING
"CLOSE" LAUNCH SUPPORT EQUIPMENT

Vehicle motion disturbed by: platform misalignment; surface wind; engine misalignment and a combination of; wind, engine and platform misalignments

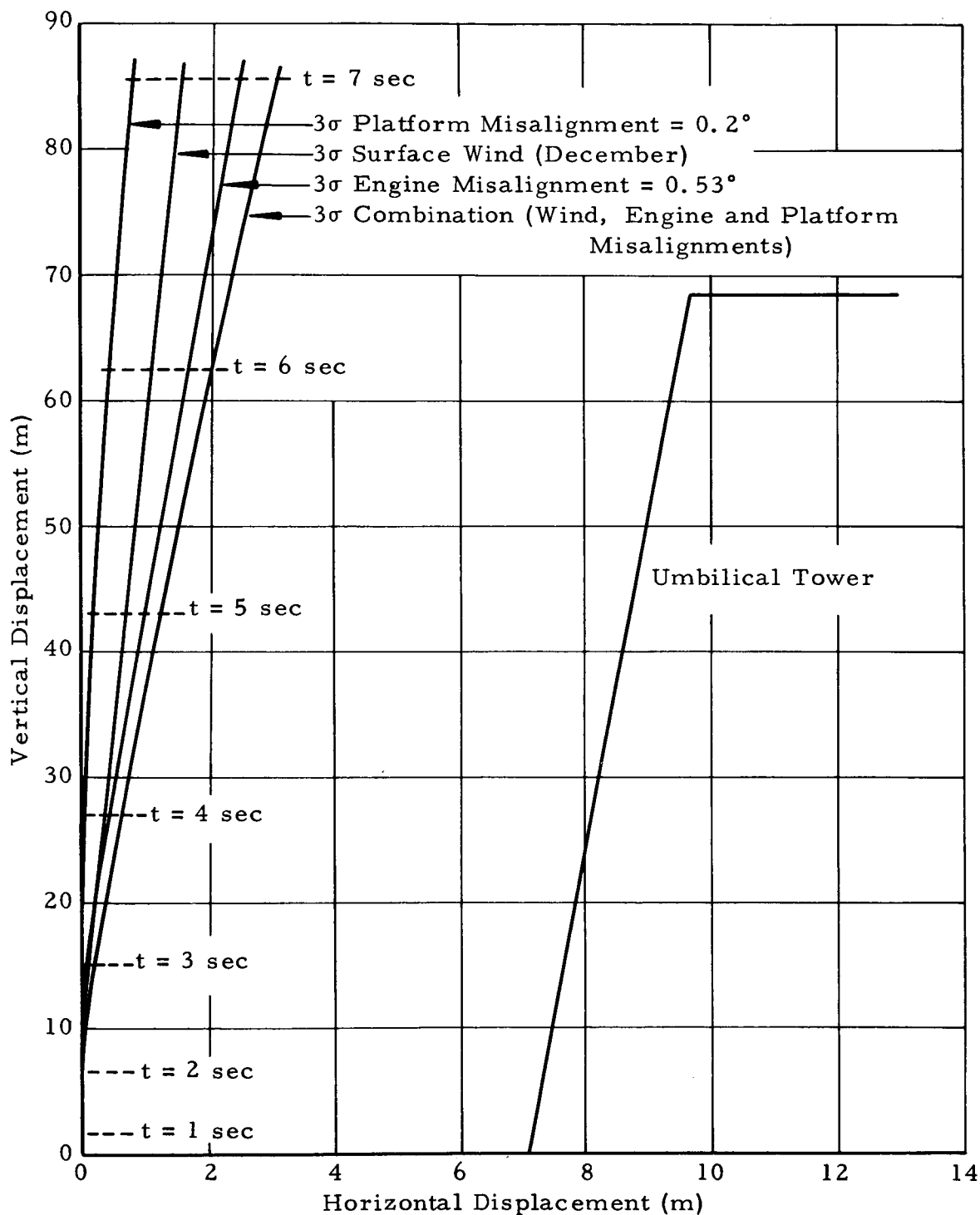


FIG. 22. TRACE OF A POINT ON FIN NO. 2

Vehicle motion disturbed by the failure of engine no. 1 at:
0, 1, 2 and 3 seconds (no other disturbances included)

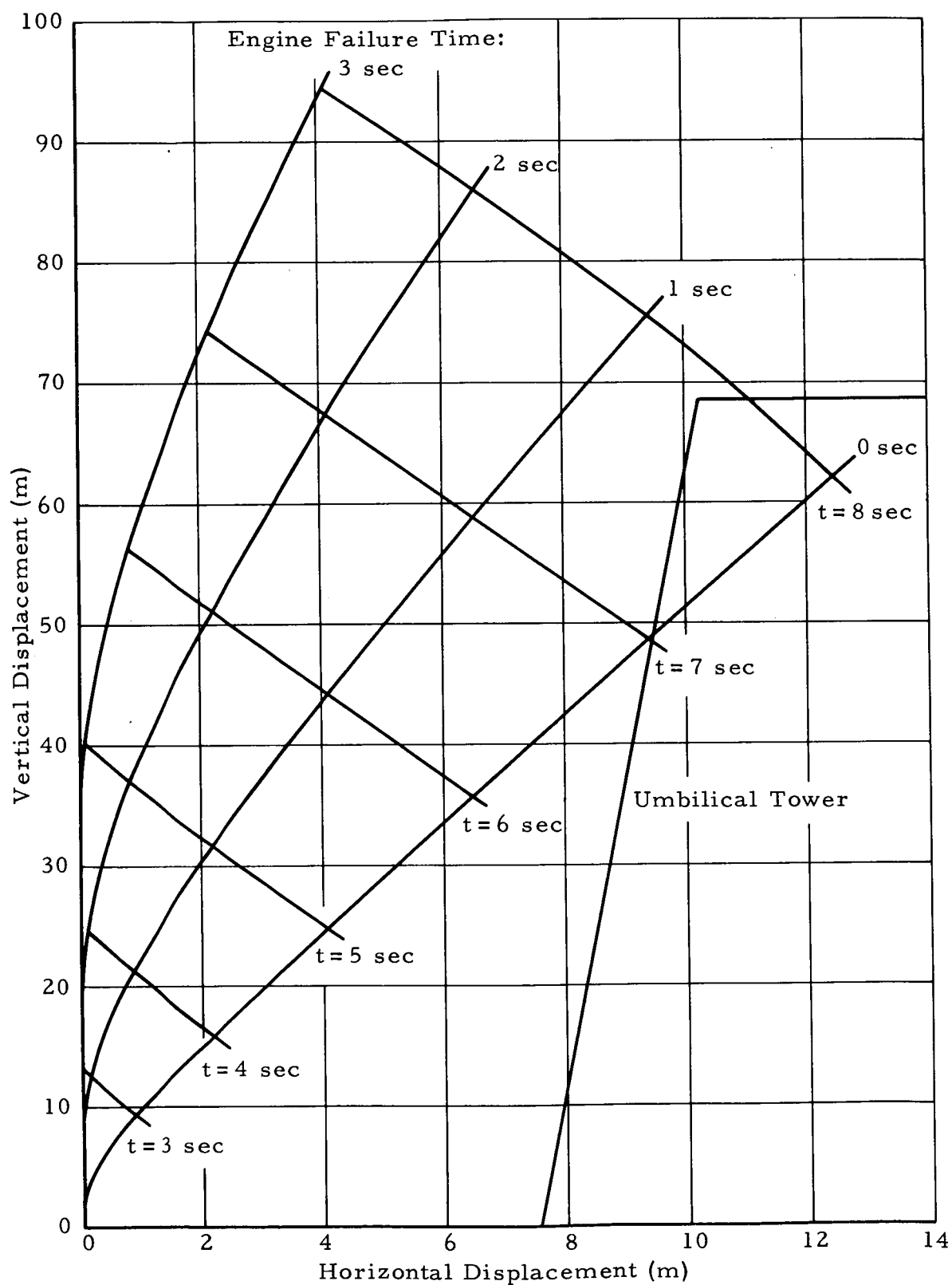


FIG. 23. TRACE OF A POINT ON FIN NO. 2

Vehicle motion disturbed by: platform misalignment; engine misalignment; wind; engine no. 1 failure at flight time, $t=0$ sec; and a combination of; platform misalignment, wind and engine misalignment

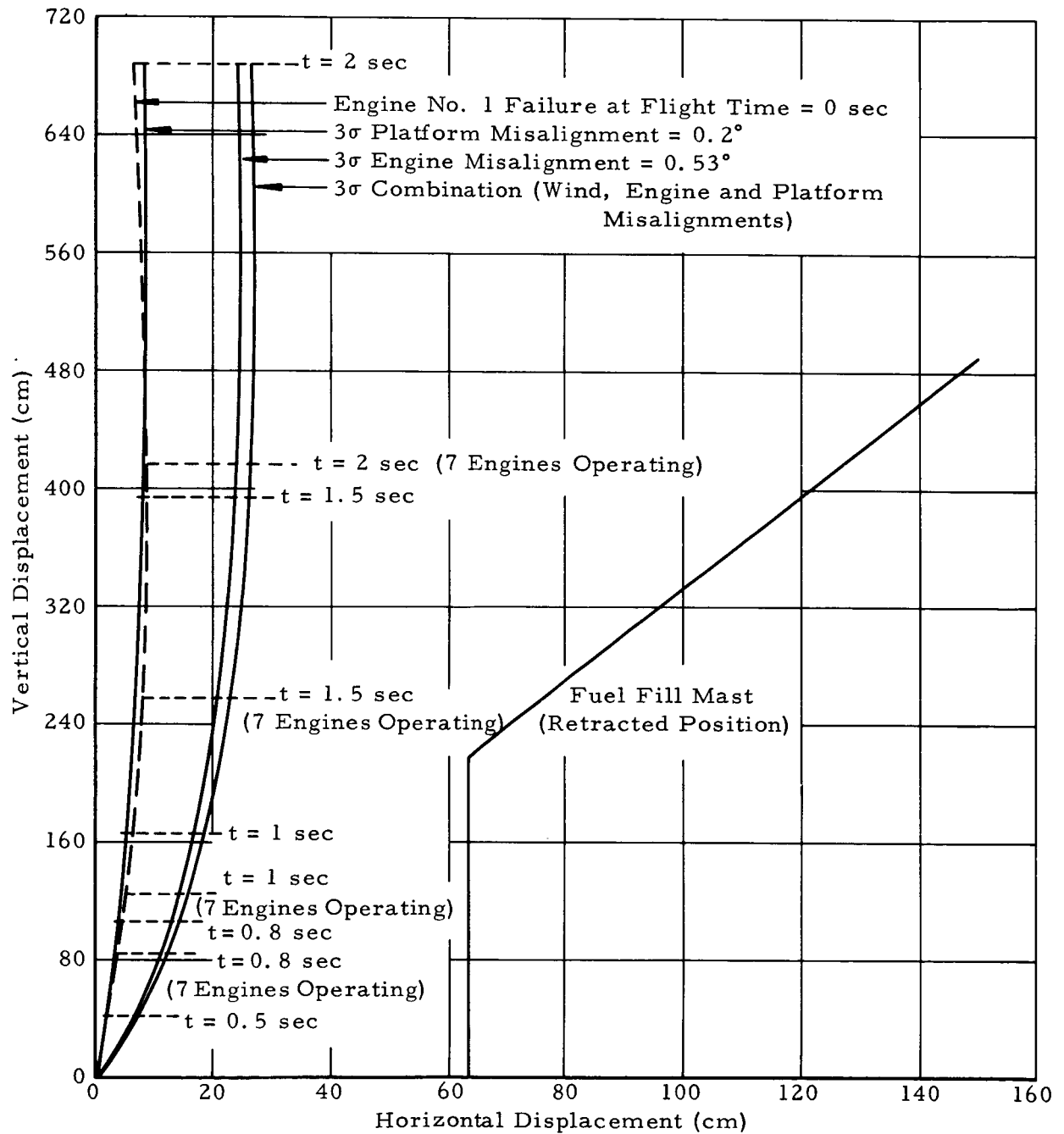


FIG. 24. TRACE OF A POINT ON INBOARD TURBINE EXHAUST DUCT ADJACENT TO FUEL FILL MAST

Vehicle motion disturbed by: platform misalignment; engine misalignment; wind; engine no. 1 failure at flight time, $t=0$ sec; and a combination of; platform misalignment, wind and engine misalignment

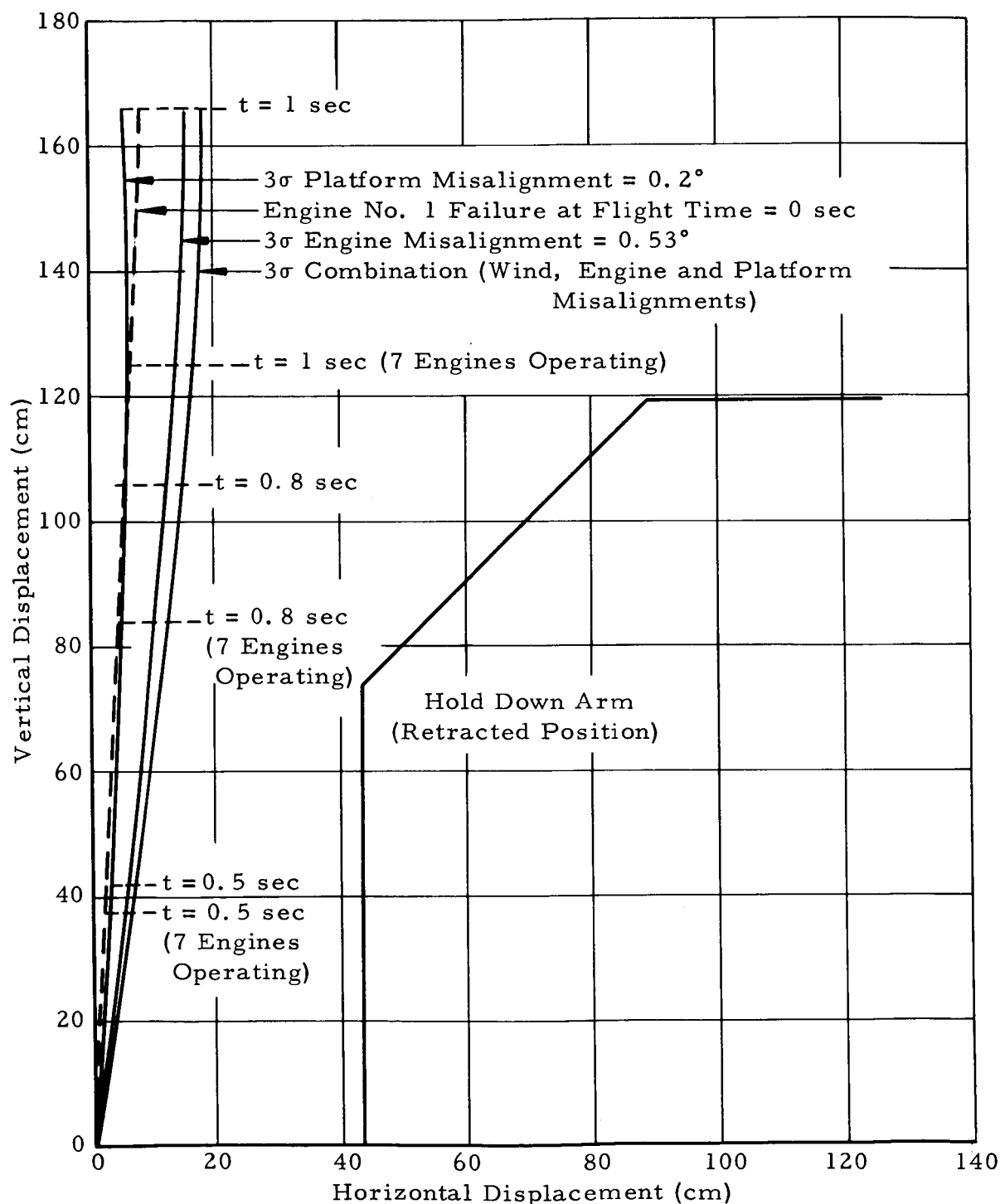


FIG. 25. TRACE OF A POINT ON SHROUD ADJACENT TO HOLD DOWN ARM

Vehicle motion disturbed by: platform misalignment; engine misalignment; wind; engine no. 1 failure at flight time, $t=0$ sec; and a combination of; platform misalignment, wind and engine misalignment

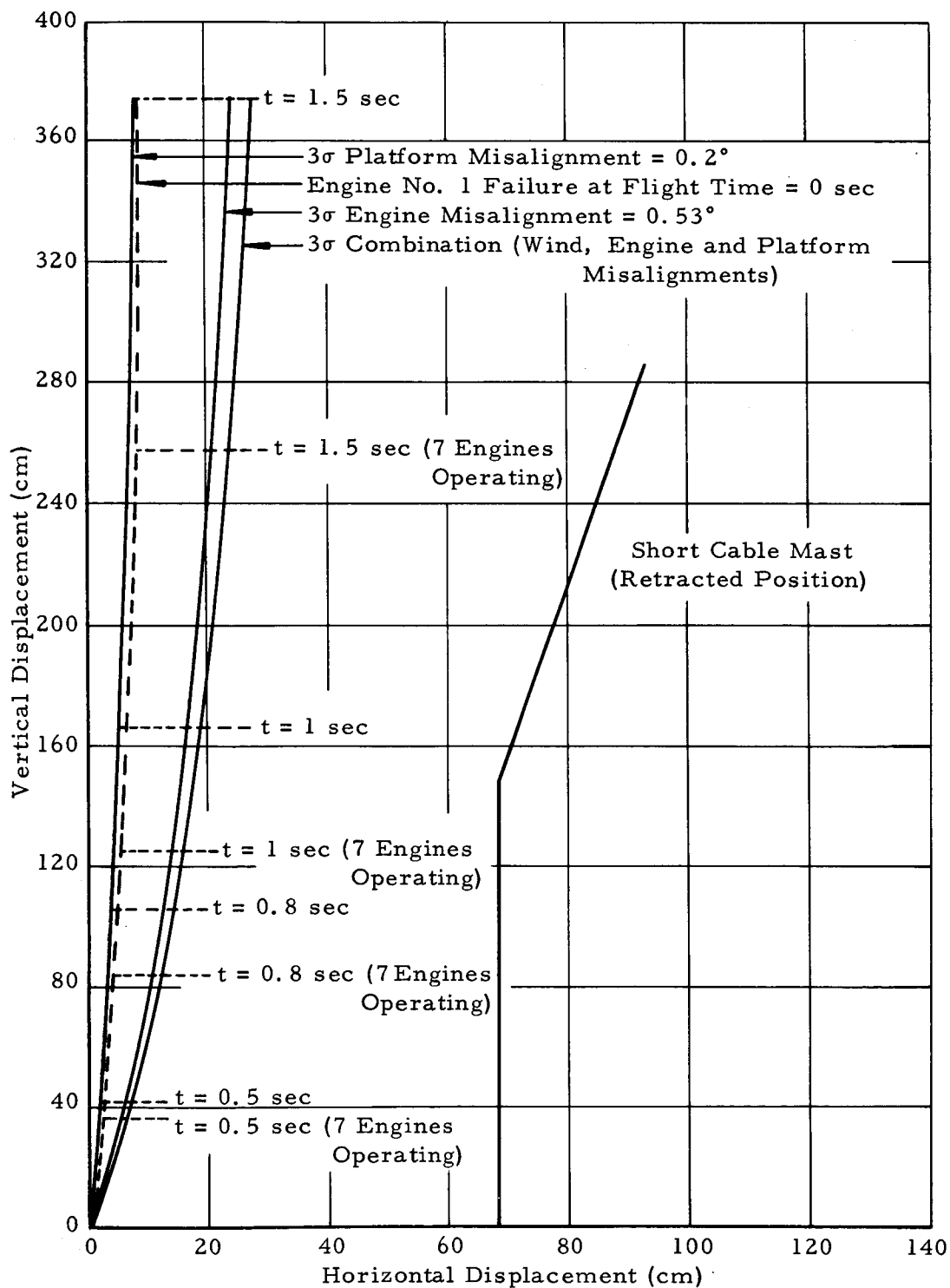


FIG. 26. TRACE OF A POINT ON SHROUD ADJACENT TO SHORT CABLE MAST

REFERENCES

1. "Rigid Body Control Study for SA-5," by E. L. Sullivan, MTP-AERO-63-73, October 23, 1963
2. "Saturn SA-6 Control Gains and Shaping Networks," by Mr. Blackstone, Flight Dynamics Branch, R-ASTR-F, November 8, 1963
3. "Control Factors for Saturn I SA-6 Vehicle," by S. A. Hopkins, Aero Internal Note No. 5-64, January 22, 1964
4. M-P&VE-EF-638, "SA-5 Flight Sequence Requirements," dated August 19, 1963
5. M-P&VE-EA-63-433, "Retrorocket Installation and Alignment at AMR for the Saturn I, S-I-5 through 10 Stages," dated September 30, 1963
6. M-ASTR-N-276, "Saturn I, Block II Alignment Tolerances Based on Navigation Requirements," dated March 27, 1963
7. M-P&VE-PP-211-63, "Predicted H-1 Engine Altitude Cut-Off Impulse for 188K Sea Level Thrust," dated May 7, 1963
8. M-S&M-PS-731, "S-I Retrorocket Altitude Performance," dated October 10, 1961
9. RL 10A-3 Engine Model Specification No. 2272B (Pratt and Whitney), dated August 15, 1962. "Thrust Information Contained in Saturn I, Block II Design Criteria Book."
10. M-P&VE-PS-397-62, Changes to Saturn Design Criteria C-1, Block II Book, S-IV Stage, December 21, 1962
11. A2-860-S-IV/G&C-M-7, "S-IV/C1 Separation, Roll Control System Recovery," dated February 7, 1963
12. M-AERO-Y, "Wind Profiles at Staging Altitudes (35 km to 80 km), dated September 27, 1961
13. M-AERO-A-53-63, "Lift-off Aerodynamic Characteristics of Saturn I, Block II Vehicles," dated June 5, 1963
14. Range Safety Data Report #2-64, "Range Safety Data for Saturn SA-6," dated April 15, 1964

APPROVAL

NASA TM X-53041

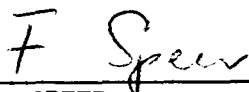
RIGID BODY STUDY OF CONTROL, SEPARATION, AND
LIFT-OFF FOR SA-6 VEHICLE

By

E. L. Sullivan, D. O. McNiel,
and W. H. Harmon

L. O. STONE

Chief, Flight Mechanics Branch



F. A. SPEER

Chief, Flt Eval & Opns Studies Division


E. D. GEISSLER

Director, Aero-Astrodynamic Laboratory

DISTRIBUTION

DIR, Dr. von Braun	R-P&VE-DIR, Mr. Cline
DEP-T, Mr. Rees	R-P&VE-DIR, Mr. Hellebrand
DEP-A, Mr. Gorman	R-P&VE-P, Mr. Paul
	R-P&VE-AVA, Mr. Denton
R-AERO-DIR, Dr. Geissler	R-P&VE-VS, Mr. Schulze
R-AERO-DIR, Mr. Jean	R-P&VE-S, Mr. Kroll
R-AERO-A, Mr. Dahm	R-P&VE-SL, Mr. Showers
R-AERO-AT, Mr. Wilson	R-P&VE-S, Mr. Hunt
R-AERO-AD, Mr. Linsley	R-P&VE-AVP, Mr. Belew
R-AERO-A, Mr. Holderer	R-P&VE-PTD, Mr. Hastings
R-AERO-D, Mr. Horn	R-P&VE-V, Mr. Palaoro (2)
R-AERO-D, Mr. Baker	
R-AERO-DD, Mr. Winch	K-V, Dr. Gruene
R-AERO-DD, Mr. Ryan	K-EF3, Mr. Hershey
R-AERO-F, Dr. Speer (2)	K-VT, Mr. Moser
R-AERO-F, Mr. Lindberg	K-VG3, Mr. Chambers
R-AERO-FF, Mr. Sheats	K-EF4, Mr. Varnadoe
R-AERO-FM, Mr. Stone	K-VE, Mr. Davidson
R-AERO-FM, Mr. Hardage	K-VG4, Mr. Jenke
R-AERO-FM, Mr. Sullivan (5)	K-VG4, Mr. Whiteside
R-AERO-FM, Mr. McNiel	K-VE, Mr. Williams
R-AERO-G, Dr. Hoelker	K-VM, Mr. Pickett
R-AERO-P, Mr. McNair	K-DIR, Dr. Debus
R-AERO-P, Mr. Teague (7)	K-T, Dr. Knothe
R-AERO-T, Mr. Reed	K-EP, Mr. White
R-AERO-T, Mr. Cummings	K-ED, Dr. Bruns
R-AERO-Y, Mr. Vaughan	K-SF, Mr. Moore
	K-ED4, Mr. Jelen
R-COMP-DIR, Dr. Hoelzer	
R-TEST-DIR, Mr. Heimbarg	CC-P, Mr. Wofford
R-ME-DIR, Mr. Kuers	MS-IP
	MS-IPL (8)
	MS-H
R-QUAL-DIR, Mr. Grau	
	HME-P
R-ASTR-DIR, Dr. Haeussermann	Scientific and Technical Information
R-ASTR-I, Mr. Hoberg	Facility (25)
R-ASTR-F, Mr. Blackstone	ATTN: NASA Representative (S-AK/RKT)
R-ASTR-R, Mr. Taylor	P. O. Box 5700
R-ASTR-FO, Mr. Mink	Bethesda, Maryland
R-ASTR-G, Mr. Mandel	
R-ASTR-NGI, Mr. Blanton	MSC-ASPO, Mr. R. E. McKann
R-ASTR-F, Mr. Hosenthien	MSC-PE-3, Mr. C. H. Perrine, Jr.
R-ASTR-N, Mr. Moore	MSC-FOD, Mr. J. P. Mayer
R-ASTR-M, Mr. Boehm	MSC-STO, Mr. J. Funk
R-ASTR-TJ, Mr. Brandner (2)	MSC-ASPO-SCE, Mr. T. H. Skopinski
R-ASTR-E, Mr. Fichtner	